USE OF SOLID PHASE EXTRACTION FOR PRECONCENTRATION OF RARE EARTH ELEMENTS: PROVENANCE STUDIES IN ÇATALHÖYÜK OBSIDIANS

A THESIS SUBMITTED TO
THE GRADUATE SCHOOL OF NATUREL AND APPLIED SCIENCES
OF
THE MIDDLE EAST TECHNICAL UNIVERSITY

BY

SEMA ÖZTÜRK

IN PARTIAL FULFILLMENT OF THE REQUIREMENTS FOR THE DEGREE
OF
MASTER OF SCIENCE
IN
THE DEPARTMENT OF CHEMISTRY

SEPTEMBER 2003

Approval of the Graduate School of Natural and Applied Sciences.

_____

Prof. Dr. Canan ÖZGEN

Director

I certify that this thesis satisfies all the requirements as a thesis for the degree of Master of Science.

_____

Prof. Dr. Teoman TİNÇER

Head of Department

This is to certify that we have read this thesis and that in our opinion it is fully adequate, in scope and quality, as a thesis for the degree of Master of Science.

_____

Prof. Dr. O. Yavuz ATAMAN

Supervisor

Examining Committee Members

Prof. Dr. Şahinde DEMİRCİ _____

Prof. Dr. Emine Caner SALTUK _____

Prof. Dr. Mürvet VOLKAN _____

Prof. Dr. O. Yavuz ATAMAN _____

Assist. Prof. Nusret Ertaş _____

ABSTRACT

USE OF SOLID PHASE EXTRACTION FOR PRECONCENTRATION OF RARE EARTH ELEMENTS: PROVENANCE STUDIES IN ÇATALHÖYÜK OBSIDIANS

Öztürk, Sema

M.S., Department of Chemistry

Supervisor: Prof. Dr. O. Yavuz Ataman

September 2003, 61 pages

Obsidian has been a center of interest both for geologists and archaeologists. Geologists have studied on physical and chemical properties of obsidian where archaeologists have worked on this material as a common artifact found in excavations.

In this study, obsidian samples from Çatalhöyük excavations are examined using their rare earth element (REE) concentrations. Inductively Coupled Plasma-Optical Emission Spectrometry (ICP-OES) have been used for this purpose. A mixture (4:1) of lithium metaborate and lithium tetraborate was used for fusion of samples. Because of the low concentrations of REEs, a preconcentration step is needed. Successful recovery results have been achieved with Amberlite IR-120.

The developed method is tested using the standard reference material SARM-1.

Keywords: Çatalhöyük, obsidian, rare earth elements, preconcentration, provenance, inductively coupled plasma – atomic emission spectrometry,

ÖZ

NADİR TOPRAK ELEMENTLERİNİN ÖNZENGİNLEŞTİRİLMESİNDE KATI FAZ EKSTRAKSİYONUNUN KULLANILMASI: ÇATALHÖYÜK OBSİDYENLERİNDE KAYNAK BELİRLEME ÇALIŞMALARI

Öztürk, Sema

Yüksek Lisans, Kimya Bölümü

Tez Yöneticisi: Prof. Dr. O. Yavuz Ataman

Eylül 2003, 61 sayfa

Obsidiyen buluntuları arkeolog ve jeologlar için ilgi kaynağı olmuştur. Jeologlar fiziksel ve kimyasal özelliklerini araştırırken, arkeologlar ise kazılarda bulunan malzeme olarak obsidyene ilgi göstermişlerdir.

Bu çalışmada, Çatalhöyük kazılarından alınan obsidiyen örnekleri nadir toprak elementlerinin derişimleri yönünden incelendi. Bu amaçla indüktif eşleşmiş plazma - optik emisyon spektrometrisi (ICP-OES) kullanıldı. Örnekler, eritiş yöntemiyle ve 4:1 oranında lityum metaborat ve lityum tetraborat karışımında çözüldü. Örnekler içerisindeki nadir toprak elementlerinin derişimlerinin düşük olması nedeniyle ön zenginleştirme basamağına gerek duyulmuştur. Amberlite-IR120 reçinesi ile başarılı sonuçlar alındı.

Geliştirilen yöntem standart referans madde (SARM-1) kullanılarak denendi.

Anahtar kelimeler: Çatalhöyük, obsidyen, nadir toprak elementleri, önzenginleştirme, kaynak belirleme, indüktif eşleşmiş plazma - atomik emisyon spektrometrisi.

Dedicated to My Family…

ACKNOWLEDGEMENTS

I would like express my deep appreciation and gratitude to my supervisor Prof. Dr. O. Yavuz Ataman for his never-ending guidance, understanding, encouragement and friendship throughout this study.

I thank to Dr.Tristan Carter of Stanford University for selecting and preparing the obsidian samples.

I would like to thank to Prof. Dr. Mürvet Volkan, Assoc. Prof. Dr. Ahmet Emin Eroğlu and Prof. Dr. Nur Balkan Atlı for their contribution during the study.

Regarding ICP-MS analyses, I would like to thank Mr. Selami Solmaz, Mr. Ahmet Öğüt, Ms. Ayse Çakır, Ms. Naime Solmaz from İzmir Hıfzıssıhha Institute as well as Ms. Aslı Erdem.

Special thanks go to Dr.Gülay Ertaş, İ. Ayhan Aysal and Z. Süleyman Can for their endless help in ICP work and their valuable discussions.

I would like to thank all my friends in Analytical Chemistry Group for their friendship and kind support.

I also thank the examining committee members for their valuable contributions to my thesis.

Finally, I would like to thank my family for their endless support and to my husband for long nights spent in the laboratories and his logistic supports.

TABLE OF CONTENTS

LIST OF TABLES

Table

LIST OF FIGURES

Figure

CHAPTER I

INTRODUCTION

1.1. Obsidian

1.1.1. Definition of Obsidian

Obsidian is a natural glass of volcanic origin, that is formed by rapid cooling of certain types of lava, which have a content of silica, greater than 65% as SiO_2. Obsidian generally contains less than 1% of water by weight. Under high pressure in depth, lava may contain up to 10% of water, which helps to keep them fluid even at a low temperature. Eruption to the surface, where pressure is low, permits rapid escape of this volatile water and increases the viscosity of the melt. Increased viscosity impedes crystallization, and the lava solidifies as glass. Different obsidians are composed of a variety of crystalline materials [1].

1.1.2. Physical Characteristics of Obsidian

Obsidian has a glassy luster and is slightly harder than window glass. Obsidian is normally shiny in appearance, and dark in color (black or gray), but sometimes colorless, red, green, or brown, depending on the composition and circumstances of formation [2]. It has a hardness of 6 on the Mohs scale and has a specific gravity of about 2.4 and a refractive index of about 1.5 [3].

1.1.3. Chemical Classification of Obsidian

Chemical classification of obsidians can be made through their oxides of aluminum, calcium, sodium and potassium contents. Peralkaline obsidians are those with greater amount of Na_2O plus K_2O than Al_2O_3, while the subalkaline

obsidians have less amount of Na_2O plus K_2O than Al_2O_3. Peraluminous obsidians have greater amount of Al_2O_3 than CaO plus Na_2O and K_2O, while metaluminous obsidians have less aluminum or aluminum oxide than CaO plus Na_2O and K_2O. Within these divisions calc-alkaline and alkaline obsidians have, respectively, high CaO and alkalis, and high alkalis (but low calcium) relative to SiO_2 [2]. Table 1.1 shows this classification.

Table 1.1 Classification of Obsidian.

Peralkaline	$Na_2O + K_2O > Al_2O_3$
Subalkaline	$Na_2O + K_2O < Al_2O_3$
Peraluminous	$Na_2O + K_2O + CaO < Al_2O_3$
Metaluminous	$Na_2O + K_2O + CaO > Al_2O_3$

According to the weight percentage of silica (SiO_2), as done in igneous rocks, obsidians can be classified in a different manner. Those with more than 66% are generally termed acidic, between 66% and 52% intermediate, between 52% and 45% basic and less than 45% ultrabasic [3].

1.1.4. Importance of Obsidian Provenance Studies

Being a very hard material, obsidian is suitable for manufacture of tools. It has been used for producing weapons, implements, and ornaments by Neolithic men. Moreover, it can be traded over long distances. Because of these properties, some obsidians are found on excavations of ancient cities. In addition, chemical composition of obsidians vary with the lava where it was formed [3].

The purpose of obsidian analysis is to establish characteristics of each sources which will serve to distinguish it from other sources. Artifacts found in archaeological sites can be examined with the same criteria, and the source of the material can be identified. This procedure, which furnishes valuable information for early prehistoric trade, is that of characterization. The method of trace element analysis has provided the most promising approach to the problems of obsidian [5] .

1.1.5. Çatalhöyük Excavations

The Çatalhöyük settlement, on the 52 km. southeast of Konya and north of the town Cumra is dated back to 6800-5000 BC (Neolithic Age) and is the most developed center of the Near East and the Aegean [6].

Çatalhöyük was first excavated in 1960s by James Melleart and those excavations uncovered dramatic evidence of elaborate decoration, such as plastered relief animals and possible divinities on wall faces and a range of wall paintings, some depicting scenes of hunting and other activities on twelve building levels which enlighten the Neolithic Age in Central Anatolia. By the near east standards, the inventory was poor, however rich for its microlithic obsidian samples and the clay objects [7].

Çatalhöyük comprises two distinct mounds, where mounds are built up by human activities. The main or east mound covers the 13.5 ha and is almost entirely Neolithic in date, with some areas of Hellenistic, Roman and Byzantine settlement. The smaller west mound covers 8.5 ha and is largely Chalcolithic, again with some much later occupation.

When the Neolithic inhabitants of Çatalhöyük built a house they did not intend it to last forever. After about a hundred years or so they would demolish their house and use the remains as the foundation for a new building. In this way the level of the settlement gradually rose over the centuries until it reached the height seen today [8].

The impact of discoveries at Çatalhöyük was immense that the previous excavations did not suspect the existence of Neolithic Age. Çatalhöyük covers a very long period with at least fourteen successive settlements, where buildings are made of mud brick, wood and plaster without stone foundations and on a rectangular plan.

1.1.6. Obsidian Analysis

Color, fracture, translucency, specific gravity, refractive index, density are properties investigated in the early scientific studies. Today, these properties are not useful themselves but combined with the chemical analysis results they can give valuable information.

By the developing technology, considerable applications in archaeological studies have been found with instrumental methods.

Abbes et al. studied on the obsidians, collected from the Jerf El Ahmar village of Syria dated 9500 BC. The elementary composition of 44 obsidian artefacts and of 19 samples from potential obsidian volcanic sources was determined by inductively coupled plasma –atomic emission spectrometry and –mass spectrometry (ICP-OES/-MS) or proton induced X-ray emission (PIXE) and scanning electron microscope-energy dispersion of X-rays (SEM-EDX). The study announces that each of these approaches gave a reliable assignment. The analysis proved that 42 of obsidians came from Cappodocia Göllü Mountain area and two from Bingöl area [9].

Chataigner et al. studied on geological samples, used for provenance studies of 112 artefacts from Armenian prehistroric sites or of pebbles from river banks which are located in Armenia and in adjacent regions of Turkey and Georgia. The analysis made by Fission-Track (FT) dating method better constrained the history of Plio-Pleistocene volcanism of this region [10].

Duttine et al. studied by electron spin resonance on about seventy obisidians coming from six Mediterranean volcanic islands. The complex spectra is mainly due to different states of iron and site location (sometimes to Mn^{+2}). X-Band (9 GHz) spectra exhibit a signal at g=4.3 with a shoulder to isolate Fe^{+3} in the glassy matrix with a rhombic environment. After than, condensated clusters of Fe^{+3} ions give rise to a resonance line at g=2.0 whose position and width do not depend on temperature; in addition to this signal, broad resonance lines are ascribed to micro-crystallines of mixed iron oxides. When temperatures are decreased from

300K to 5K, this signals shift towards weak fields and the contribution of every signal to Electron Spin Resonance (ESR) differs from one source to another [11].

Oddone et al. studied the application of instrumental and epithermal neutron activation analysis to the obsidian occurrences from Northern, Central and Eastern Anatolia. Their results include 39 element composition of different obsidian sources from Anatolia [12].

Fission track dating technique is a complementary technique that was used in the provenance studies of obsidians. When the chemical composition is not suitable to reveal the source of obsidians, the age may be useful [4].

In another work, Bellot-Gurlet et al. have coupled proton induced X-ray emission (PIXE) with fission track dating to characterize obsidian artefacts from about 40 archaeological sites of Colombia and Ecuador. Hundreds of analyses prove that fusion track dating is a complementary technique which turns out to be very useful especially when the chemical composition does not fully discriminate different sources [13].

Another method, particle induced gamma-ray emission (PIGE), was applied for the analysis of source material of obsidians of archaeological use. The authors also compared PIGE with the laser ablation-inductively coupled plasma- mass spectrometry (LA-ICP-MS) [14].

1.2. Rare Earth Elements

1.2.1. History of Rare Earth Elements

The term Rare Earth was suggested by Johann Gadolin in 1794. They were called rare earth originally because when they were first discovered they were thought to be present in the earth's crust only in small amounts and they were isolated as oxides (in old usage "earth" mixtures). The numerous chemical similarities between the REEs means that it took more than a century from the

first discovery to complete isolation and classification. Compared to calcium and magnesium they are rather rare, but more abundant in the earth's crust then many of the more familiar elements such as lead, zinc, tin, mercury, iodine, bromine, silver, gold and platinum. The term rare earth elements refers to the 14 elements following La (Lanthanum) (Z=57, $[Xe]4f^0$) to Lu (Lutetium) (Z=71, $[Xe]4f^{14}$) in the periodic table. Since the 4f electrons are relatively uninvolved in bonding, these highly electropositive elements have their prime oxidation number as +3, resemble one another chemically and physically [15,16].

Rare earth elements are classified in two groups:

- The light or cerium subgroup, comprising the first seven elements, Z=57-63, Lanthanum (La), Cerium (Ce), Praseodymium (Pa), Neodymium(Nd), Promethium (Pm), Samarium (Sm), Europium (Eu).
- Heavy or yttrium subgroup, comprising the elements Z=64-71, Gadolinium (Gd), Terbium (Tb), Dysprosium (Dy), Holmium (Ho), Erbium (Er), Thulium (Tm), Ytterbium (Yb), Lutetium (Lu).

1.2.2. Abundance and Occurrence of Rare Earth Elements

There are more than 200 minerals which are sufficiently rich in these elements to serve as practical sources of rare earths. Significant production of REEs began in the 1880s, with mining of the mineral monozite in Brasil.

Monazite, $[(Ce,La,Nd,Th)\ (PO_4)]$ which occurs as a dense, brown sand, is particularly rich in the light rare earths. Bastnaesite, a fluorocarbonate and Xenotime, a phosphate mineral, are the most economically significant minerals containing essential or significant rare earth elements [17]. Bastnaesite and monazite are sources of rare earths about 95% of the rare earths currently utilized. Monozite is also a principle ore of thorium (Th) containing up to 30% ThO [18].

The largest rare earth element mineral deposites are found in Scandinavia, Brasil, Australia, India, Russia and the United States. Bastnaesite is mined

mainly in California and provides most of the 35 to 40 x 10^3 tones of RE oxides used annualy.

1.2.3. Determination of Trace Rare Earth Elements

Determination of REEs in geological, biological and environmental samples is one of the most difficult and complicated tasks, especially at trace levels, because of the similarity of their chemical behaviors.

Moreover, these samples provide diverse matrices that are exceptionally complex both chemically and physically. The complexity of such samples raises the possibility that interelement effects of various types or spectral interference may introduce errors in determination of REEs. Since the REEs are usually present in very small concentrations (at or below μg/g levels) in samples, separation of these elements as a group should be incorporated in the analysis. The separation not only allows for preconcentration of the REEs so that lower detection limits are possible, but also simplifies the analytical problem of interference from matrix elements, when samples in a varying compositions are encountered [19].

The most widely used techniques for separation and preconcentration of trace REEs include coprecipitation, liquid-liquid extraction, solid-phase extraction, HPLC and ion exchange.

Roychowdhury et al. reported the oxalate precipitation technique for preconcentration of REEs in silicate rocks. After the oxalate precipitate was formed, they were ignited to the oxide, which is then dissolved in dilute nitric acid [20].

Srivastava and Premadas studied on liquid-liquid extraction involving the mixture of (2-Ethylhexyl) dihydrogenphosphate and (2-Ethylhexyl) hydrogenphosphate in kerosene for separation and preconcentration of REEs in acidic solutions of silicate rock samples. The REEs are selectively stripped from the organic phase

containing interfering elements using 4.5M hydrochloric acid in the presence of tri-n-butyl phosphate [21].

In the recent years, solid-phase extraction (SPE) has become increasingly popular. Numerous substances have been proposed and applied as sorbents, such as modified silica, alumina, active carbon, cellulose, chelating resins and microorganisms. Several examples are given in the following paragraphs.

Halicz et al. succeed in separation of REEs from the saline water by adsorption on a micro-column of silica-immobilized 8 –hyroxiquinoline. After adsorption on the micro-column at pH 9, the REEs are eluted with a small volume of the mixed diluted hydrochloric and nitric acids [22].

Biosorption is a potential purification process for sequestering metallic cations from diluted aqueous solutions. Metal sorption on the cell surfaces can occur in non-living microorganisms. Texier et al. immobilized a microorganism, Pseudomonas aeruginosa, in poliacrylamide gel as a biosorbent for the removal of REE ions from aqueous solutions. In this study, for the desorption of REEs from the biosorbent particles 0.1M EDTA (pH 5.0) was used [23].

As an effective technique for separation and preconcentration of trace elements, solid-liquid extraction with microcrystalline naphthalene has received great attention in recent years. This technique is based on the distribution of analyte between the solid and liquid phases. Cai et al. reacted tribromoarsenazo (TBA), extremely sensitive reagent for REEs, with REEs to form the water soluble complexes, and the REE complexes formed were transformed into water-insoluble ion-associated complexes in the presence of the counter-ion reagent cetylpyridinium bromide, which can be easily adsorbed onto microcrystalline naphthalene at ambient temperature. The analytes were desorbed with hydrochloric acid [24].

Chelating resins are frequently used in analytical chemistry for preconcentration of metal ions and their separation from interfering constituents prior to their determination by an instrumental method. The selectivity of chelating resin is

often related to that of the monomeric compound corresponding to the functional group. Dev et al. prepared a polystyrendivinylbenzene (Amberlite XAD-4) based chelating resin containing bicine (n,n-bis(2-hydroxyethyl)glycine) groups. The batch equilibration technique was used to concentrate the metal ions. A sample solution was adjusted at optimum pH=6 and shook with resin. Sorbed metal ions were eluted with 1M hydrochloric acid [25].

Roelandts used Dowex 50-WX 8 cation exchange resin for the preconcentration and separation of REEs. 8M nitric acid was used as an eluent solution. The REEs eluent was slowly evaporated to dryness and the residue was dissolved in 5% nitric acid [26].

1.3. Ion Exchange Resins

Ion exchange has been defined as reversible exchange of ions between the solid and liquid in which there is no substantial change in the structure of the solid. In an ion exchange resin one of the ionic species is always mixed high polymer network and therefore remains insoluble or immobile in the solid phase. The oppositely charged ion is mobile and can exchange or swap with other cations in the ambient solutions.

Ion exchange resins are high molecular weight polyacids or polybases which are virtually insoluable in most aqueous or non aqueous media. They may be pictured as having structures containing large polar exchange groups held together by a three dimensional hydrocarbon network. Cation exchangers can contain sulfonic, phosphorous, phosphoric, carboxylic or phenolic groups. Anion exchangers can contain primary, secondary and tertiary amine groups and quaternary ammonium groups [17].

In the beginning of 19 th century, ion exchange was primarily the significance of the process in the field of agricultural chemistry. Most investigations are carried out with clays and minerals, among them zeolites had great interests. The technical production of material similar to the zeolites is based on work by Gans

which was published in about 1905. The synthetic zeolites are mainly used for the softening of water [27].

In 1917, Folin and Bell used ion exchange for the determination of ammonia in urine. This reaction can not be made directly by adding Nesslers reagent, as certain amino acids interfere. It was found that, on shaking the solution with a synthetic zeolite, ammonia was taken up whereas interfering elements remained in the solution. The ion exchanger was separated and after treatment with sodium hydroxide the liberated ammonia was determined according to the Nessler method.

1.3.1. Amberlite IR-120

Amberlite IR-120 contains crosslinked polystyrenes with sulfonic acid groups which have been introduced after polymerization by treatment with concentrated sulfuric or chlorosulfonic acid [28].

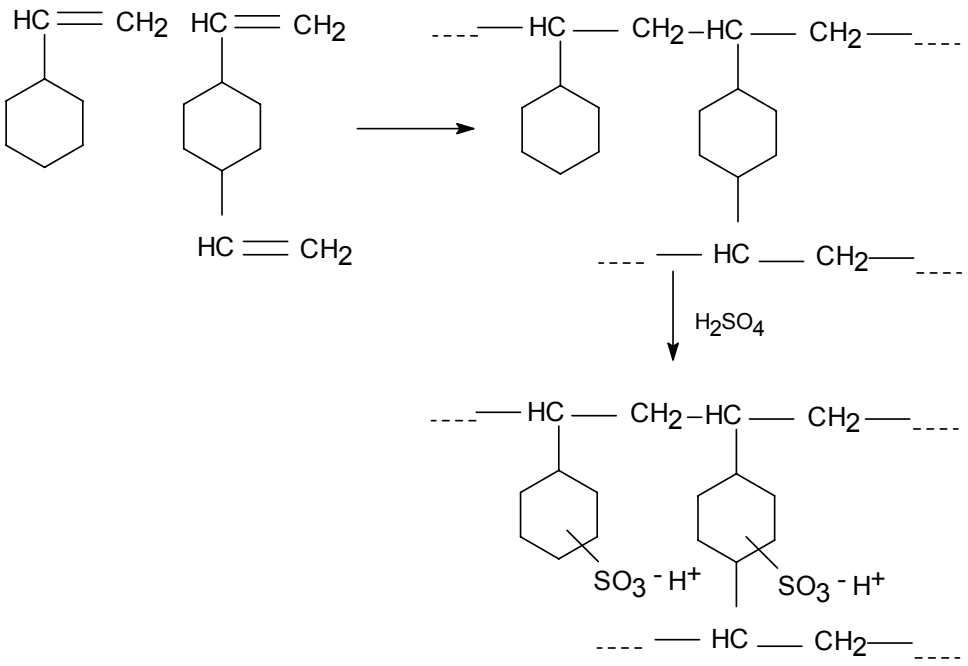

Figure 1.1 Open Structure of Amberlite IR-120 [28]

1.4. Inductively Coupled Plasma-Atomic Emission Spectrometry

The Inductively coupled plasma (ICP) was first studied as an analytical emission source in the early 1960s by Fassel and coworkers in United States (Iowa State University) and by Greenfield and coworkers in United Kingdom (Albright and Wilson Ltd.). The first commercial ICP spectrometer was introduced in 1975, more than 10 years after the first description of ICP sources. Since that time, there was a phenomenal growth in the number of ICP spectrometers in scientific laboratories [29].

The plasma methods provide some of the most useful and spesific means for the determination of the REEs at trace levels. High sensitivity, multielement analysis capability, speed of analysis and high reproducibility are the advantages of ICP-OES technique. Having high energy, ICP permit the determination of elements that tend to form refractory compounds, that is compounds that are highly resistant to decomposition by heat. Regarding REEs determinations, ICP-OES is significantly superior to AAS. Even though the chemical properties of various lanthanides are very similar, the spectra of these elements are just as unique as those of other elements [30].

ICP-OES is the most popular and widely used multielement technique, either with or without preconcentration, for determination of individual REEs in metallurgical, environmental and geological samples [31].

1.4.1. Robustness of ICP-OES

The robustness of an ICP-OES instrument is the capability of its system to accept a change in the concentration of major elements, acids and other elements without any significant variation in the line intensity of the analytes [28]. The use of robust conditions provide more reproducible ICP conditions.

When axial viewing is used, the entire central channel is probed. Therefore, matrix effects may be more important than radial viewing. Because the

atomization zone located within the coil is then probed by the observation system which is not the case with radial viewing. It appears that axially-viewed plasma may be more sensitive to matrix effects than radially viewed plasmas. Use of robust conditions could minimize but not necessarily suppress matrix effects when ionic lines are of concern [32] .

Robustness of conditions can be verified by measuring the intensity ratio of an ionic to atomic spectral line of the same element [33]. Experimental ionic to atomic line intensity ratios allow an evaluation of departure from Local Thermodynamic Equilibrium (LTE) but also they reflect any inefficiency in the atomization, excitation and ionization process [34].

To analyze the robustness conditions, MgII (280.270 nm.) / MgI (285.213 nm.) ratio were used in literature. (In atomic spectroscopy, MgII refers to the ionic line of Mg and MgI refers to the atomic line of Mg) For the selection of the element, the observed criteria are shown below:

- Closeness of the excitation energies of the atomic and ionic lines, 35051 cm^{-1} (MgII 280.270 nm.) and 35669 cm^{-1} (MgI 285.213 nm.) .
- High sensitivity to plasma parameter change (the sum of the ionization energy and the excitation energy in the range 11-13 eV. are the most sensitive lines to any change in the energy transfer between the plasma and the injected species) [34].
- The intensities of the ionic and atomic lines are of the same magnitude [32].

The ideal case is observed when there is both no change in the MgII/MgI ratio and analyte signal. A common case is no change in the MgII/MgI ratio but a change in the analyte signal. This means that plasma conditions were not changed, usually because of robust conditions, but the variation in the analyte signal can be explained by problems that arise at the aerosol transport and filtration level.

Experimentally measured magnesium ion to atom ratios and electron densities were used to determine the deviation of plasma from LTE conditions. The Saha

distribution determines the ion to atom population ratio for a species as a function of ionization temperature. The following equation relates the ionization temperature of a species to the experimentally observed ion to atom emission intensity ratio.

$$\frac{I^+}{I^o} = \frac{2(2\pi m_e kT)^{3/2} g^+ A^+ \lambda^o}{n_e h^3 \quad g^o A^o \lambda^+} \exp(-\Delta E/kT)$$

where I^+ and I^o are the intensities for the ionic and atomic emissions, g^+ and g^o are the statistical weights of the upper states involved in the emissions, A^+ and A^o are the Einstein transition probabilities, λ^o and λ^+ are the wavelengths of the ionic and atomic emissions, k is the Boltzmann constant, h is the Planck's constant, m_e is the mass of an electron, ΔE is the energy difference between the upper state of the atomic transition and the upper state of the ionic transition, n_e is the electron density and T is the ionization temperature.

By using g, A values [6], I^+/I^o value must be at least 10, so the plasma could be in equilibrium. The ratio above 10 indicates that the ICP should not be particularly sensitive to matrix effects, where as the ratio below 4 corresponds to high sensitivity to matrix effects. For the ratios below 4, careful matrix matching of the unknown and standard solutions must be carried out [35].

However, the experimental results for MgII/MgI ratio have different radial and axial modes. In the radial mode, the MgII/MgI ratios are measured in the optimum observation height corresponding to the optimum ionic line emission. In contrast, when the axial viewing mode is used both atomic line and ionic line emission zones are probed by the collimating system resulting to lower MgII/MgI ratio than the radial viewing even if the same ICP operating conditions are used [32] .

Ionic to atomic line ratios can be increased by changing the operation parameters of ICP-OES such as carrier gas flow rate, power and observation height (for

radial viewing). Higher power values give higher MgII/MgI ratio. Higher carrier gas flow rates gives lower MgII/MgI ratio [32].

It is known that some matrices of easily ionizable elements (such as K and Na) and other elements (such as HNO_3 , H_2SO_4) to cause analyte signal suppression or enhancement in ICP-OES [33].The plasma becomes more and more sensitive to the presence of Na when moving to non-robust conditions. In particular, atomic lines were found to be sensitive to the presence of elements such as Na, Li, and Ca even under so called robust conditions. To eliminate this problem, an alternative way is the use of a buffer. The buffer is an element present at high concentration whose influence would predominate over the influence of other elements such as Na or Li. A consequence would be that a change in the concentration of Na or Li would cause no effect on the plasma conditions. Cs, having the lowest ionization energy (3.894 eV.), emits only a few lines and usually cannot be determined in ICP-OES because of poor sensitivity. That is why, Cs would be a good buffer. The presence of Cs decrease the value of MgII/MgI ratio, but made it possible to keep this ratio constant for the Na concentration changes [32].

1.5. Aim of the Study:

The main purpose of this study was the preconcentration and recovery of some REEs elements and secondly to analyze obsidian samples from Çatalhöyük excavations in order to find out the sources of obsidians artifacts. 50 obsidian samples from east mound of Çatalhöyük were examined to reveal the rare earth element composition, 4 elements (La, Ce, Nd, Sm) were determined by ICP-OES. For provenance of samples, the results was statistically evaluated.

CHAPTER II

EXPERIMENTAL

2.1. Chemicals and Reagents

i) 1000mg Lanthanum / L standard solution (in dilute HNO_3) : Ultra Scientific

ii) 1000 mg Cerium / L standard solution (in dilute HNO_3) : Ultra Scientific

iii) 1000 mg Neodymium / L standard solution (in dilute HNO_3) : Ultra Scientific

iv) 1000 mg Samarium / L standard solution (in dilute HNO_3) : Ultra Scientific

v) Amberlite IR-120(plus) ion-exchange resin : Aldrich Chemical Company

vi) 1018 mg Magnesium / L standard Solution (in dilute HNO_3): Aldrich Chemical Company

vii) $LiBO_2$: JMC 10/3 Specpure)

viii) $Li_2B_4O_7$: J.T.Baker, Flux Grade

ix) Nitric Acid : Carlo Erba, reagent, 65% (w/w)

x) Hydrochloric Acid : Merck, analysis grade, 36% (w/w)

Amberlite IR-120 is a strongly acidic cation exchange resin. It has styrene divinylbenzene copolymer matrix with sulphonic acid functional groups [36].

Table 2.1 Properties of Amberlite IR-120

Physical form	Amber beads
Ionic form	H
% Moisture	45%
Total exchange capacity	1.9 meq/mL
pH range	0-14
Max. operating temperature °C	120

The method development process of the preconcentration procedures was performed and tested by using certified reference material, SARM 1, granite sample produced by South African Bureau of Standards. The certified concentrations of the components were given in Table 2.2.

Table 2.2 Certified values in SARM 1.

Element	Concentration (μg/g)
Lanthanum	109 ± 5
Cerium	195 ± 8
Neodymium	72 ± 8
Samarium	15.8 ± 1.8

Durapore Membrane Filter, with 0.45 μm pore size, manufactured by Millipore were used through all filtering processes.

Milli-Q Deionized water, which has a Milli-Q 18 MΩ.cm resistance, was obtained by water purification system fed by Electro deionization system Millipore Elix-5.

2.2. Instrumentation and Apparatus

For the determination of La, Ce, Nd, Sm concentrations in obsidian samples, Leeman DRE ICP-OES instrument was used. The instrument employs a photomultiplier tube (PMT) as detector and allows the use of the facility of sequential multi-element analysis. An axial plasma torch was used. Burgener

2002 Meinhardt type nebulizer was used in sample introduction system of ICP-OES. The operating parameters of the instrument throughout the study were given in Table 2.3.

Table 2.3. Plasma conditions for ICP-OES, Leeman DRE.

Rf Power	1.4 kW
Nebulizer Gas	36 Psi
Auxiliary Gas	0.5 LPM
Coolant Gas	16 LPM
Pump Rate	0.7 mL/min

Nuve SL350 shaker was used for all shaking processes.

The Pt crucibles used in dissolution procedures contains 5% Au. The dissolution was continued in PTFE beakers and all dilutions were performed using polypropylene volumetric flasks.

At the end of each working period, the crucibles and beakers were cleaned in 10 % HNO_3 by heating on a hot plate for about 30 min. The volumetric flasks were allowed to wait in 10 % HNO_3 at least for a night. All materials were rinsed using pure water before use.

2.3. Samples

During the summer of 1999, 50 pieces of obsidian were selected for the pilot-study to be conducted at METU. These samples were selected by archeological team led by Dr. Tristan Carter on the basis of their physical properties (colour, texture, inclusions) and their archaeological context. The material all came from the South Area of the East mound, focusing on deposits from Levels VIII-X excavated in 1999. Details of samples are given in Table 2.4.

Table 2.4. Details of obsidian samples from Çatalhöyük*

Sample No.	Mound	Area	Building	Space	Unit	Level	Description
OB 51 (99)	East	South		115	4121	VIII	Flake
OB 52 (99)	East	South		115	4121	VIII	Flake
OB 53 (99)	East	South		115	4121	VIII	Flake
OB 54 (99)	East	South		115	4121	VIII	Flake
OB 55 (99)	East	South		115	4121	VIII	Flake
OB 56 (99)	East	South		115	4102	VIII	Blade frag.
OB 57 (99)	East	South		115	4102	VIII	Flake
OB 58 (99)	East	South		115	4102	VIII	Flake
OB 59 (99)	East	South		115	4102	VIII	Flake
OB 60 (99)	East	South		115	4121	VIII	Blade frag.
OB 61 (99)	East	South		115	4121	VIII	Blade frag.
OB 62 (99)	East	South		115	4121	VIII	Flake
OB 63 (99)	East	South		115	4121	VIII	Blade frag.
OB 64 (99)	East	South		115	4121	VIII	Blade frag.
OB 65 (99)	East	South		115	4121	VIII	Blade frag.
OB 66 (99)	East	South		115	4121	VIII	Flake
OB 67 (99)	East	South		115	4121	VIII	Flake
OB 69 (99)	East	South		115	4121	VIII	Flake
OB 70 (99)	East	South		115	4121	VIII	Blade frag.
OB 71 (99)	East	South		115	4121	VIII	Flake
OB 72 (99)	East	South		115	4121	VIII	Flake
OB 73 (99)	East	South		115	4121	VIII	Blade frag.
OB 74 (99)	East	South	2, 9	117, 166	4209	IX, X	Flake
OB 75 (99)	East	South	2, 9	117, 166	4209	IX, X	Flake
OB 76 (99)	East	South	2, 9	117, 166	4209	IX, X	Flake

(Table 2.4 Continued)

OB 77 (99)	East	South	2, 9	117, 166	4209	IX, X	Flake
OB 78 (99)	East	South	6	163	4280	VIII	Flake
OB 79 (99)	East	South	2	117	4138	IX	Flake
OB 80 (99)	East	South	2	117	4138	IX	Blade frag.
OB 81 (99)	East	South	2	117	4138	IX	Flake
OB 82 (99)	East	South	2	117	4138	IX	Flake
OB 83 (99)	East	South	2	117	4138	IX	Blade frag.
OB 84 (99)	East	South	2	117	4138	IX	Flake
OB 85 (99)	East	South	23	178	4987	X	Flake
OB 86 (99)	East	South	23	178	4987	X	Flake
OB 87 (99)	East	South	23	178	4989	X	Flake
OB 88 (99)	East	South	23	178	4989	X	Flake
OB 89 (99)	East	South	23	178	4989	X	Flake
OB 90 (99)	East	South	23	178	5103	X	Flake
OB 91 (99)	East	South	23	178	5103	X	Flake
OB 92 (99)	East	South	23	178	5103	X	Flake
OB 93 (99)	East	South	23	178	5103	X	Flake
OB 94 (99)	East	South	23	178	5103	X	Flake
OB 95 (99)	East	South	23	178	5087	X	Flake
OB 96 (99)	East	South	23	178	5095	X	Blade frag.
OB 97 (99)	East	South	23	178	5095	X	Flake
OB 98 (99)	East	South	23	178	5095	X	Flake
OB 99 (99)	East	South		115	4121	VIII	Blade frag.
OB 100 (99)	East	South		115	4121	VIII	Blade frag.

*The terms and descriptions in Table 2.4 were given by the autority of Çatalhöyük excavation and kept here for archiving purposes.

In this study, 29 out of 50 obsidians were analyzed because of low amount of some samples.

The obsidian samples were powdered by breaking down with a hammer between two steel sheets, the formed particles were sampled.

2.4. Procedures

2.4.1. Dissolution by Fusion

Sample was dissolved by fusion with two reflux materials, $LiBO_2$ and $Li_2B_4O_7$. Three replicate measurements were performed by the following way: 0.200 g of sample was weighed and placed into the crucible. 1 g of $LiBO_2$-$Li_2B_4O_7$ mixture (4:1) was added to the crucible and all the solid material was mixed with a PTFE rod. The same procedure was followed for the blank solution.

The crucibles were heated in a muffle furnace at 1050°C for 1 hour. The fused glass was cooled and transferred into a PTFE beaker. The beaker was placed on magnetic stirrer after adding about 100 mL water and 2.5 mL of concentrated HNO_3. The crucible was rinsed with 5 mL of 20 % HNO_3 and the contents were poured into the beaker. A watch glass is used to cover the beaker and the contents were stirred until all the melt is dissolved. The dissolution took about 2-3 hours. Any undissolved part was examined during the dissolution process. The solution was diluted to 250 mL in a plastic volumetric flask, so the final concentration of HNO_3 becomes 1%. This procedure was used also for dissolution of SRM samples.

2.4.2. Optimization for Performance of the Amberlite IR-120 in Preconcentration of Rare Earth Element Species

For all solutions, used in optimization experiments, SARM-1 standard reference material (SRM) was used and it was prepared according to the procedure mentioned in section 2-4.

2.4.2.1. Uptake and Recovery for High REE Concentrations

2.4.2.1.1. Uptake Values

In order to find optimum time required for sorption of La, Ce, Nd and Sm by resin, 10 mg/L La, Ce, Nd and Sm were spiked into the 20 mL of SRM solution and mixed with 0.2 g Amberlite IR-120 resin. The solutions were shaken for various periods of time. Then, they were filtered through membrane filter under vacuum and the filtrates were analyzed for determining the percent uptake for each shaking period.

2.4.2.1.2. Recovery Values

After collection of La, Ce, Nd and Sm on Amberlite IR-120 resin (take up), the recovery of La, Ce, Nd and Sm from the resin was studied. For this purpose, 20 mL of the 10 mg/L of La, Ce, Nd and Sm in SRM solutions are prepared and mixed with 0.2 g Amberlite IR-120 resin. Mixtures shaken for 1.5 hour for take up were filtered and Amberlite IR-120 resins left on filter paper were taken into 20 mL HCl solutions in various concentrations for recovery. They were shaken with these HCl solutions for 30 minutes. The resin was filtered and filtrates were analysed for their La, Ce, Nd and Sm content.

2.4.2.2. Uptake and Recovery Values for true REE Concentrations

2.4.2.2.1. Effect of Elution Acid Volume on Recovery

To find out the minimum acid amount for elution of all REE species from resin, SRM solutions prepared with the procedure mentioned in section 2.4. were shaken with 1 g Amberlite IR-120 resin for 12 hour. After filtration, resins were transferred into another container and hydrochloric acid solutions in various volumes were added into the resins. The eluents were analyzed for their REE contend.

2.4.2.2.2. Effect of Multiple Elution

To increase the recovery values, SRM solutions prepared with the procedure mentioned in section 2.4. were shaken with 1 g of Amberlite IR-120 resin for 12 hours. After filtration, resins were transferred into another container. Initially, the elution acid was used in one aliquot.

Secondly, the elution acid was divided into two parts of equal volumes. The first aliquot of acid was added onto resin and the contents were shaken for 30 minutes. After the filtration process, the filtrate was stored in another container. The second aliquot of acid was added onto the same resin and the contents were shaken again for 30 minutes and then filtered. The two filtrates were combined.

Finally, the above process was repeated by dividing the total acid volume into three equal portions.

2.4.2.2.3. Uptake Values

In order to find original concentrations of REEs in SRM solutions, uptake time was optimized. For this purpose, SRM was dissolved as mentioned in section 2.4; 1 g of Amberlite IR-120 was added into solution and the mixture was shaken for various time periods. After filtration from membrane filter under vacuum, resin particles were transferred into another container and a measured volume of 6 M HCl solution was added. The contents were shaken for 1 hour and filtered. La, Ce, Nd and Sm content of filtrates were determined by ICP-OES.

2.4.2.2.4. Effect of Resin Amount on Recovery

To find out the optimum resin amount that gives the highest recovery values, 250 mL SRM solution prepared with procedure mentioned section 2.4. were shaken with various amount of Amberlite IR-120 resin for 4 hour. The solutions were filtrated and resins transferred into another container. 15 mL, 6 M HCl was used as eluent.

2.4.2.2.5. Effect of pH and Cations on Recovery

To understand the resin behavior to REEs in higher pH values, the pH of the SRM solution, prepared according to the procedure in the section 2.4., was tried to be increased by using NaOH, KOH and NH_3 solutions. 3 mL of NH_3 (conc.), 2.35 mL KOH (1.3 M) or 2.75 mL NaOH (1.3M) were used to increase pH of 100 mL SRM solution to 2.5.

In order to find the effect of added cations during the base addition, solutions containing increasing amount of Na^+, K^+ or NH_4^+ and 5 mg/L La were prepared in distilled water. 0,2 g of Amberlite IR-120 resin was added into solutions and they were shaken for 4 hours. After filtration from membrane filter, La concentration of solutions was determined by ICP-OES.

2.4.2.2.6. Effect of Acid Percentage in Dissolution Process on Recovery

In order to understand effect of HNO_3 concentration on recovery, 0.2 g of SRM was fused with 1g $LiBO_2$-$Li_2B_4O_7$ mixture (4:1). Glassy material formed after fusion was transferred into PTFE beakers containing 100 mL deionized water and various amounts of HNO_3. The solutions were diluted into 250 mL and 1 g of resin added into them before shaking for about 4 hours. After filtration, resins were taken into another container and they were shaken with 6M HCl for 1 hour. They were filtered and La, Ce, Nd and Sm contents were determined.

2.5. Quantitative Analysis

La, Ce, Nd and Sm contents of SRM and obsidian samples were determined by ICP-OES. The wavelengths were chosen in interference free spectral regions with appropriate sensitivity for the concentration values obtained after preconcentration. Table 2.5 shows the wavelengths used in the analysis. After completion of the analysis, the data were transferred to Microsoft Excel prior to processing.

Table 2.5 Chosen wavelengths for REE in ICP-OES, Leeman DRE.

Element	Wavelengths (nm)
La	408.672
Ce	418.660
Nd	415.608
Sm	359.827

The SRM and obsidian samples were also analysed in İzmir Hıfzıssıhha Institution by ICP-MS (Agilent 7500) for their REE contents. All elements were determined by using original solutions. The selected interference free isotopes can be seen in Table 2.6. Ytterbium was used as internal standard during experiment.

Table 2.6 Chosen isotopes for REE in ICP-MS, Agilent 7500.

Element	Isotopes
La	139
Ce	140
Nd	146
Sm	147
Y	89

2.5.1. Robustness of ICP-OES

To examine the robustness of ICP-OES instrument in different time periods, MgII/MgI ratio experiments were performed. For this purpose, 5 mg/L Mg solution was prepared. Their intensities in two different Mg line were measured in 30 minute time period.

2.5.1.1. Effect of Li on Robustness

Solutions having different amounts of lithium metaborate-lithium tetraborate were fused in 1000°C as in the procedure mentioned in section 2.4 paragraph 2. 5 mg/L Mg was spiked into the solution and Mg line intensities are measured by ICP-OES.

CHAPTER III

RESULTS AND DISCUSSION

3.1. Dissolution Process of Obsidian

The different dissolution methods were examined by Ayhan Aysal in his M.S. thesis [37] and it was found that fusion with lithium metaborate- lithium tetraborate was the most suitable method for obsidian samples. So dissolution method of obsidian was not studied in this thesis.

3.2. Robustness of ICP-OES

MgII/MgI ratio is used in literature to evaluate the robustness of ICP-OES systems. If the matrix components in a sample do not alter the characteristics of a plasma, it is called as a *robust* system. It is known that an ICP-OES system can be described as non-robust if the MgII/MgI ratio is below than 4 [35]. The found MgII/MgI ratio for our ICP-OES was 5. So we have increased the Rf power of our system from 1.1 kW to 1.4 kW and our MgII/MgI ratio was increased to 8, which shows more robust conditions.

Long term stability was proven by found MgII/MgI ratio experiments, repeated for every 30 minutes for a 7 hour period.

3.2.1. Effect of Li on Robustness

It is known that some matrices from easily ioniazable elements such as Li^+ , Na^+, K^+ have enhanced or depressive effect on plasma when moving the non-robust conditions. Because of the dissolution process, great amount of Li was introduced to the solution. For this reason effect of Li on plasma conditions was examined by the experiment mentioned below.

0.6g, 0.8g, 1g, 1.2g and 1.4 g. lithium metaborate-lithium tetraborate (4:1) was dissolved by fusion and diluted to 250 mL. After than, 5 mg/L Mg were added into the solution and MgII / MgI ratio was examined versus lithium as seen in the Figure 3.1. In the conclusion, it is seen that lithium has no effect on the robustness.

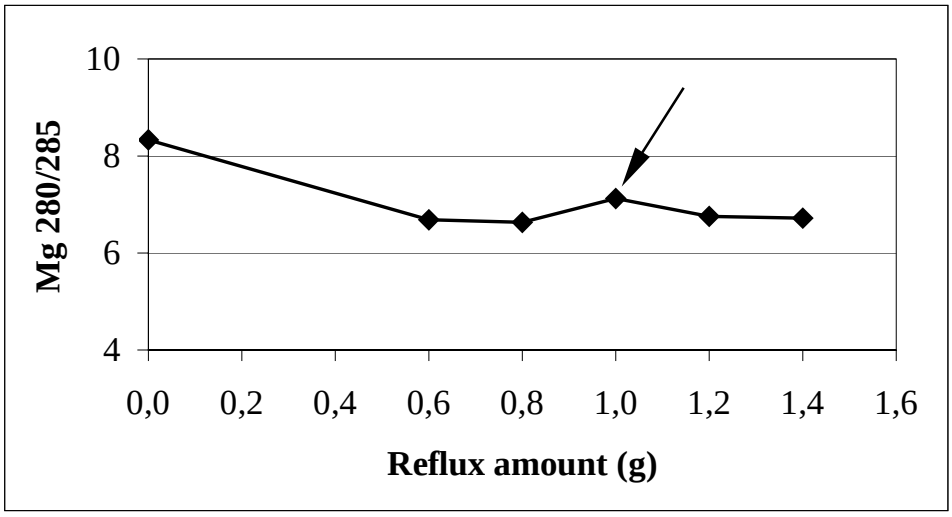

Figure 3.1 Effect of lithium flux on robustness, 5 mg/L in solutions containing various amount of reflux material.

3.3. Selection of REE

The main criteria of selection of La, Ce, Nd and Sm among the other REEs was the database [39], which was used to evaluate the results found. The only REEs

present in the database are La, Ce, Nd and Sm. Secondly, the concentration of other REEs are so low in obsidian samples that determination of them by ICP-OES with or without a preconcentration step is almost impossible. Therefore, La, Ce, Nd and Sm were selected to be determined in obsidian samples.

3.4. Selection of Resin

Several sorbents, having different functional groups, were examined for the preconcentration of REEs. For this purpose, solutions containing 10 mg/L La, Ce, Nd and Sm were shaken for 1 hour in presence of some weighed resin. After the filtration, the REE content of solutions were determined by ICP/OES.

Firstly, mercapto modified silica gel, first synthesized by M. Volkan [40], which has –SH groups were tried but the results were not good.

Secondly, another sorbent, amino sol-gel, having $–NH_3$ groups was studied. Unsuccessful uptake results were obtained again with this resin.

Then, Zeolite β was examined. The pore size of Zeolite β was suitable for REEs and resin gave successful results in neutral solutions. Unfortunately, pH of our sample solutions were too low because of the dissolution process and Zeolite β did not give successful results below pH 4.

REE have an oxyphyl character. So, a resin containing oxygen atoms were found to test. Amberlite IR-120 have $–SO_3$ as a functional group and gave successful uptake results with the REE solutions prepared in water and SARM-1 SRM solution.

3.5. Optimization for Performance of the Amberlite IR-120 in Preconcentration of Rare Earth Element Species

ICP-OES has been used successfully for the analysis of a wide range of objects. Although the detection limits of ICP-OES are very low, determination of rare earth elements in geological samples is complicated because of the low contents of REEs and significant background signals from the matrix. For this reason, a preconcentration step is necessary in this study. Moreover, a preconcentration step is a separation method resulting with a decrease in the matrix constituent.

Since most of the resins can give different behaviors with high and low concentrations, in the following section, the experiments were performed for high and low concentrations of REEs.

All solutions, used in optimization experiments, were prepared using SARM-1 standard reference material (SRM), according to the procedure mentioned in section 2.4.

3.5.1. Uptake and Recovery for High REE Concentrations

Matrix has a major effect on uptake and recovery values. So, for a successful matrix matching, rare earth element solutions were prepared by granite SRM, SARM-1, which has similar matrix to obsidian.

3.5.1.1. Uptake Values

To find out the optimum time required for sorption of La, Ce, Nd and Sm by resin, solutions containing 10 mg/L La, Ce, Nd and Sm and mixed with Amberlite IR-120 resin. The solutions were shaken for various periods of time. Then, they were filtered through membrane filter under vacuum and the filtrates were analyzed for determining the percent uptake for each shaking period.

The percent uptake vs time diagram is given in Figure 3.2.. It is seen from the figure that 90 minutes shaking gave the highest percent uptake values for each element. There is a small change between 30 minutes and 90 minutes, however for being on the safe side 90 minutes shaking was used for the recovery experiments.

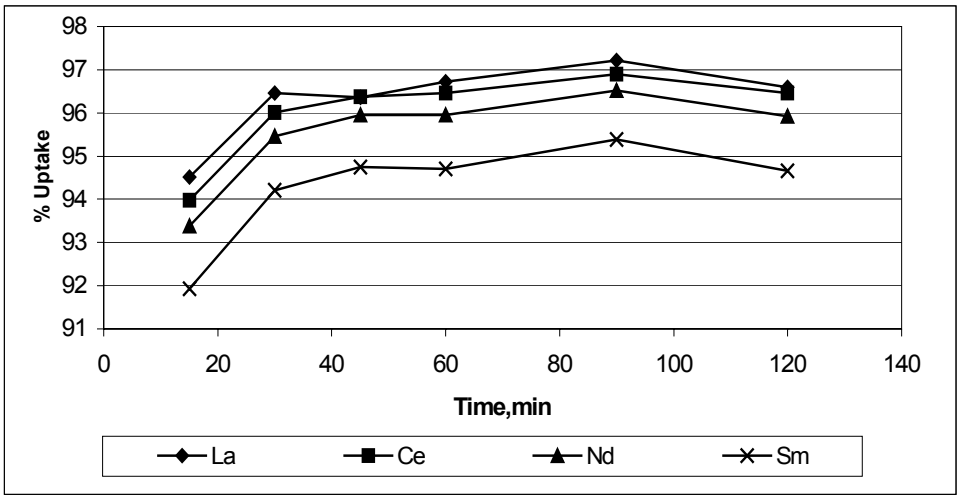

Figure 3.2 Uptake percentage as a function of time, 20 mL, SARM-1 SRM solution containing 10 mg/L La, Ce, Nd, Sm; 0.2g Amberlite IR-120

3.5.1.2. Recovery Values

During the recovery studies, 20 mL of 10 mg/L La, Ce, Nd, Sm solutions were shaken with 0.2 g of Amberlite IR-120 resin for 90 minutes. Uptake of resin was found above 90 % for each element in the solutions. To recover La, Ce, Nd, Sm species from the resin, various concentrations of hydrochloric acid were examined. % Recovery values were increased with increasing HCl concentration as can be seen in Figure 3.3. Therefore, 6 M HCl was chosen for recovery of REE species from Amberlite IR-120 resin. Since percent recovery values reached 100%, throughout the optimization experiments 6 M HCl was used.

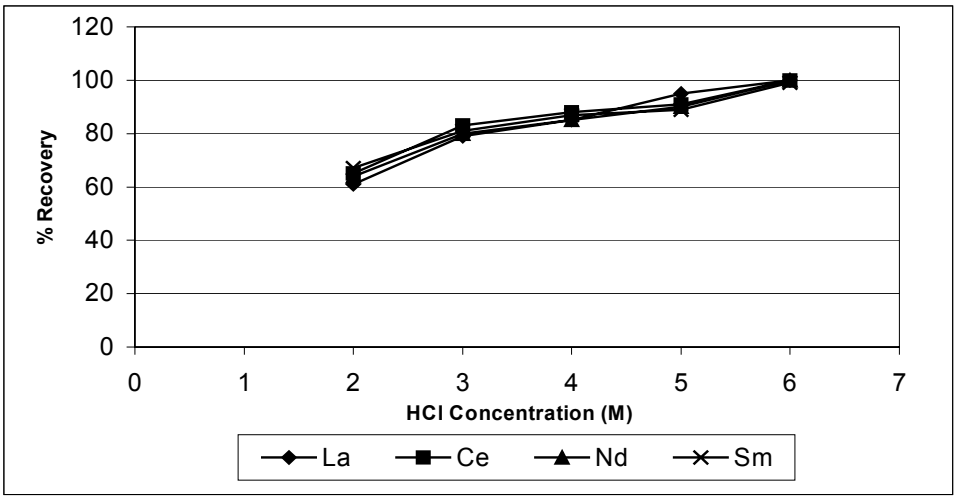

Figure 3.3 Dependence of elution on HCl concentration. 20 mL of the 10 mg/L of La, Ce, Nd and Sm were loaded; 20 mL of eluent was used.

3.5.2. Uptake and Recovery Values for True REE Concentrations

3.5.2.1. Effect of Elution Acid Volume on Recovery

It is known that, minimum eluent volume is necessary to obtain higher preconcentration factors. To investigate the minimum acid for the elution of REE species from resin, volume of elution acid were optimized. Resin shaking for four hours with SRM solution prepared according to procedure mentioned in section 2.4., were shaken with various volume of HCl for elution. It is found that 15 mL acid are enough for the recovery of REE species from resin. Figure 3.4 gives the results. Unfortunately, the preliminary recovery values were not high enough.

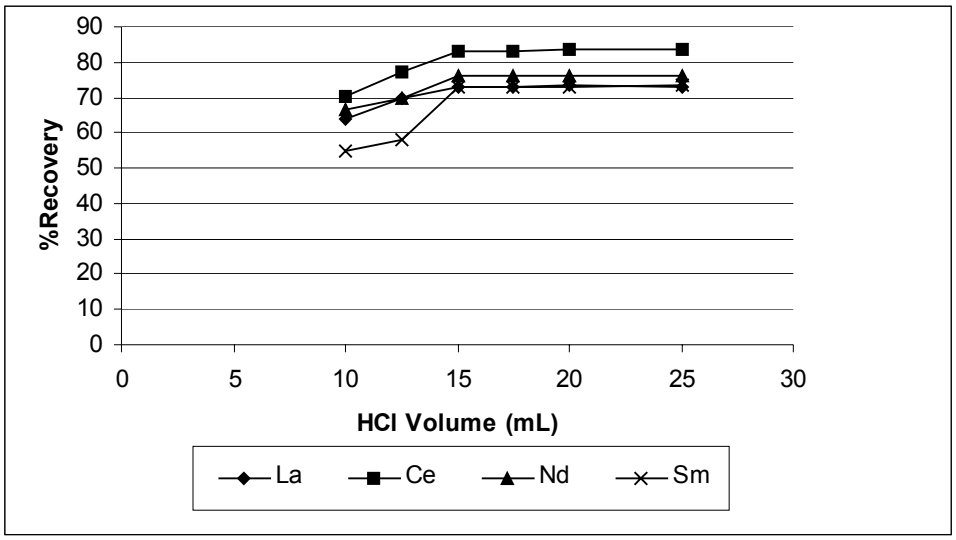

Figure 3.4 Effect of Elution Acid Volume on Recovery, 250 mL SARM-1 SRM solution, 1g Amberlite IR-120.

The preliminary studies have shown that, elution could not be completed at a single step. Therefore two and three successive elutions, dividing the total eluent volume to three equal portions of the same resin with fresh acid solution were tried. As can be seen from the Table 3.1., recoveries increased for three shakings and reached the highest value we obtained, 80-90 %.

Table 3.1. % Recovery of REE with different elution steps

Element	% Recovery Single Elution	% Recovery Two Elutions	% Recovery Three Elutions
La	63	71	98
Ce	59	66	90
Nd	58	64	87
Sm	48	54	82

Up to know, 12 hours shaking time was used for uptake step, because, it is known that uptake rates may be lower for low concentrations as compared to high concentrations, due to the slower adsorption kinetics. But the minimum

shaking time is important in order to develop a practical preconcentration procedure. Therefore, the shaking time for uptake was optimized by performing the elution step with three successive shakings. Uptake trend in low concentrations is shown in Figure 3.5. 4 hours of shaking was used for uptake in the final experiments.

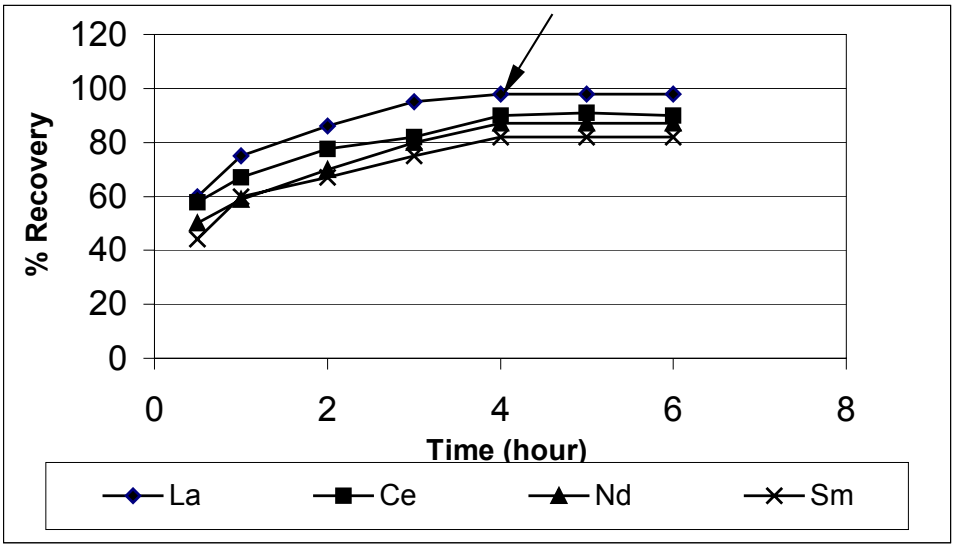

Figure 3.5 % Recovery values for true concentrations, 250 mL SARM-1 SRM solution, 1g Amberlite IR-120, 15 mL 6 M HCl.

3.5.2.2. Effect of Resin Amount on Recovery

To investigate whether the resin used in the previous optimization experiments was enough, various amounts of resin were placed into SRM solutions prepared through dissolution process as mentioned in section 2.4. and the contents were shaken for 4 hours. After filtration, elution was performed. The results can be seen in Figure 3.6. 1g resin was used in the later experiments.

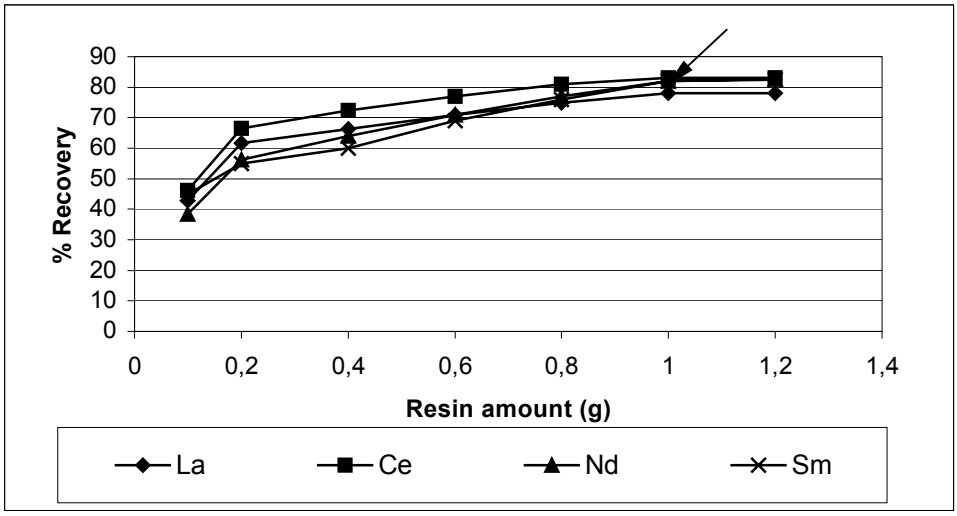

Figure 3.6 Effect of resin amount on recovery, 250 mL SARM-1 SRM solution, 1g Amberlite IR-120, 15 mL 6 M HCl.

3.5.2.3. Effect of Solution pH on Recovery

Amberlite IR-120 is a cation exchange resin. It is thought that, in low pH values, H^+ can react with resin instead of REEs, resulting with poor uptake and recovery values. Therefore, this experiment was designed to understand the effect of solution pH on recovery. For this purpose, different bases such as NaOH, KOH, NH_3 were used to increase the pH of SRM solution, SARM-1. To understand the effect of cations on uptake rates, which were formed during addition of base, cation moles was calculated. After that, solutions were prepared containing chloride salts of Na^+, K^+, NH_4^+ according to the calculated values and 5 mg/L La^{+3}. The solutions were shaken with resin and filtered. The La content of filtrates were determined by ICP-OES. The effects of Na^+, K^+ or NH_4^+ on uptake efficiency are shown in Figure 3.7,3.8 and 3.9, respectively.

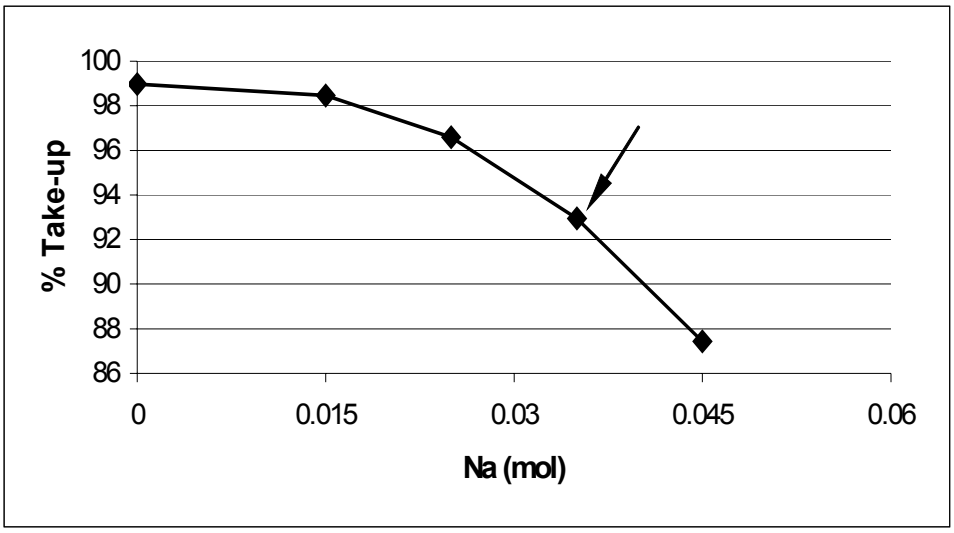

Figure 3.7 Effect of Na^+ on uptake efficiency, 5 mg/L La in distilled water, shaking time 4 hour

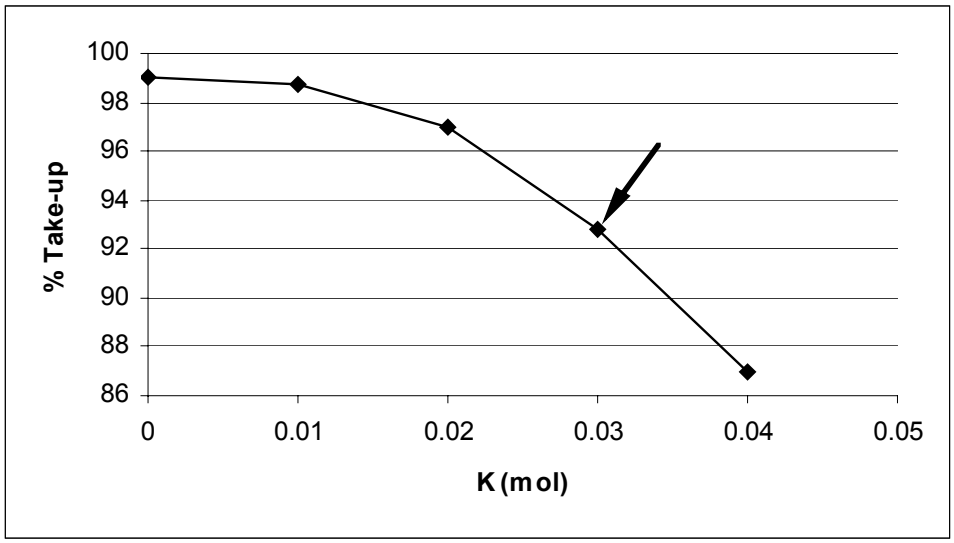

Figure 3.8 Effect of K^+ on uptake efficiency, 5 mg/L La in distilled water, shaking time 4 hour

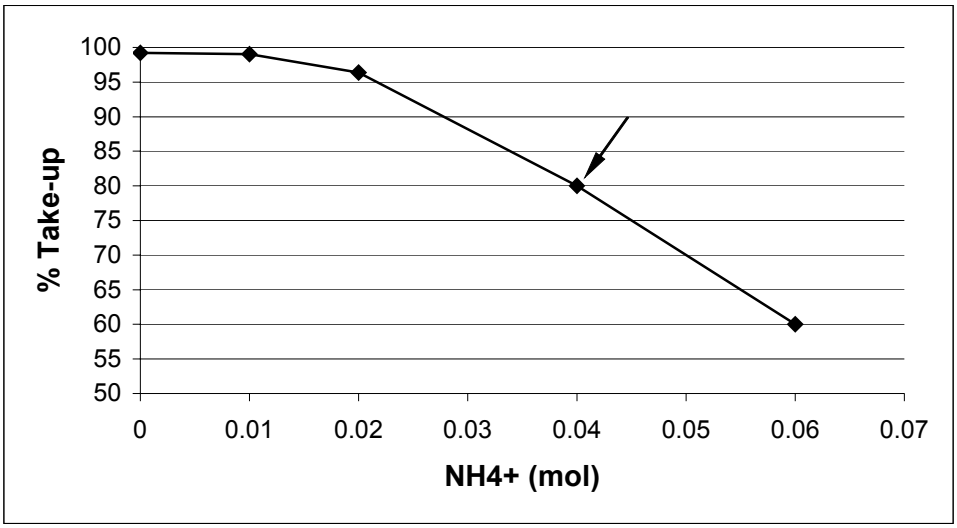

Figure 3.9 Effect of NH_4^+ on uptake efficiency, 5 mg/L La in distilled water, shaking time 4 hour

It is seen from the figures 3.7, 3.8 and 3.9 that the take up percentage decreased sharply with the cations, formed after the addition of bases. So, pH of SARM-1 SRM solution, were made higher by adding lower amount of HNO_3 in dissolution process, as explained in section 3.2.2.4.

3.5.2.4. Effect of Acid Percentage Used in Dissolution Process on Recovery

It was concluded that 5% HNO_3 was successful for the solubility of glassy material [37]. In order to investigate effect of HNO_3 amount added in dissolution process on recovery, SARM 1, was fused with $LiBO_2$-$Li_2B_4O_7$ mixture. Glassy material formed after fusion was transferred into PTFE beakers containing deionized water and various amounts of HNO_3. Firstly, it was observed that glassy material can be solved in 1% HNO_3 concentration and then the solutions were diluted into 250 mL and shaken with resin added to them. After filtration, resins were taken into another container elution step with HCl was performed.

They were filtered and La, Ce, Nd and Sm contents were determined. As it can be seen from Figure 3.10, the highest recovery results obtained by 1% HNO_3 concentration.

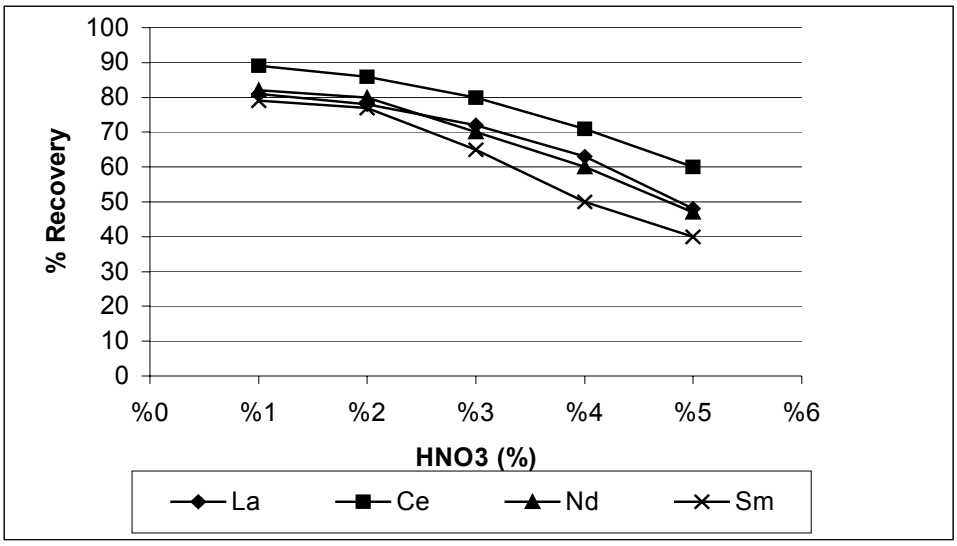

Figure 3.10 Effect of acid percentage in dissolution process on recovery, 250 mL SARM-1 SRM solution, 1 g Amberlite IR-120 resin, 15 mL 6M HCl.

After all optimization experiments, obsidian sample solutions, prepared with procedure in section 2.4.1, were shaken with 1 g Amberlite IR-120 for four hours. After the filtration, REE were eluted from resin with 15 mL 6M HCl in three step elution.

3.6. Evaluation of Results

3.6.1. Results of analysis of Reference Materials

Standard reference material 278, National Institute of Standards and Technology NIST 278 Obsidian Rock SRM was also analyzed for accuracy check. Fusion was used for dissolution of the SRM. Results are given in Table3.2.

Table 3.2 Results of SARM-1, SRM

Element	Certified values (μg/g)	Found values by ICP-OES (μg/g)	Found values by ICP-MS (μg/g)
La	109 ± 5	105 ± 2	113 ± 3
Ce	195 ± 8	167 ± 8	217 ± 2
Nd	72 ± 8	60 ± 2	78 ± 2
Sm	15.8 ± 1.8	13.2 ± 1.1	15.5 ± 0.5

Table 3.3 Results of NIST 278 Obsidian Rock SRM

Element	Recommended values (μg/g)	Found values by ICP-OES (μg/g)	Found values by ICP-MS (μg/g)
Ce	62.2	52.0 ± 0.9	66.9 ± 2.9
Sm	5.7	5.3 ± 0.6	5.5 ± 0.2

In the NIST 278 SRM, the certified values of La and Nd are not given. Only recommended values of Ce and Sm are given. Therefore SARM-1 granite SRM which has similar matrix to obsidian SRM, was used in the analysis.

3.6.2. Results of analysis of obsidian samples

29 obsidian samples were dissolved and preconcentrated as mentioned above and the solutions were analyzed with ICP-OES. 21 out of 29 obsidian samples were also analysed with ICP-MS. Results are given in Table 3.4, 3.5.

Table 3.4 Results of obsidian samples with ICP-OES (Values are in mg/kg)

	OB 52	OB 54	OB 55	OB 56
La	36.19 ± 3.37	37.73 ± 4.51	40.68 ± 0.19	40.68 ± 0.47
Ce	39.19 ± 0.80	37.47 ± 1.07	39.61 ± 0.73	38.73 ± 0.58
Nd	12.20 ± 0.71	24.21 ± 4.12	12.36 ± 0.39	12.03 ± 0.93
Sm	3.66 ± 0.80	4.28 ± 0.67	3.16 ± 0.32	2.96 ± 0.23

	OB 57	OB 58	OB 60	OB 61
La	39.70 ± 1.11	36.71 ± 1.09	35.58 ± 0.06	41.58 ± 0.36
Ce	37.44 ± 1.41	37.07 ± 2.27	34.92 ± 0.42	37.80 ± 0.40
Nd	11.99 ± 0.62	13.21 ± 0.56	11.07 ± 0.24	10.97 ± 1.08
Sm	3.13 ± 0.25	3.50 ± 0.32	3.47 ± 0.06	3.29 ± 0.09

	OB 62	OB 64	OB 66	OB 68
La	53.35 ± 1.98	36.22 ± 0.53	51.10 ± 1.53	38.35 ± 1.00
Ce	53.86 ± 1.24	33.38 ± 2.18	52.44 ± 0.32	33.75 ± 0.91
Nd	15.18 ± 0.71	9.59 ± 0.57	15.10 ± 0.55	10.55 ± 1.29
Sm	3.50 ± 0.28	3.31 ± 0.18	3.94 ± 0.08	3.63 ± 0.12

	OB 69	OB 71	OB 72	OB 74
La	44.07 ± 1.24	40.99 ± 0.78	39.07 ± 1.20	42.06 ± 0.96
Ce	37.61 ± 1.83	35.37 ± 0.61	33.95 ± 0.85	36.89 ± 0.68
Nd	10.92 ± 0.24	10.57 ± 1.19	10.00 ± 0.65	10.38 ± 0.40
Sm	3.94 ± 0.24	3.68 ± 0.25	4.43 ± 0.35	5.42 ± 0.49

	OB 75	OB77	OB79	OB80
La	42.72 ± 1.98	32.04 ± 0.52	31.75 ± 0.32	31.79 ± 0.63
Ce	35.44 ± 1.07	33.60 ± 0.36	32.57 ± 0.53	33.49 ± 0.70
Nd	10.60 ± 0.47	9.39 ± 0.46	8.94 ± 0.46	9.83 ± 0.39
Sm	4.92 ± 0.22	2.60 ± 0.17	2.73 ± 0.13	2.54 ± 0.06

	OB 81	OB82	OB87	OB90
La	29.52 ± 0.66	30.90 ± 0.33	30.03 ± 1.19	29.83 ± 0.51
Ce	31.20 ± 1.26	32.22 ± 0.37	32.38 ± 0.77	33.06 ± 0.51
Nd	9.45 ± 0.95	8.92 ± 0.11	8.66 ± 0.60	9.44 ± 0.55
Sm	2.52 ± 0.05	2.50 ± 0.17	2.75 ± 0.18	2.72 ± 0.19

	OB91	OB92	OB93	OB97
La	29.21 ± 0.45	29.22 ± 0.39	29.55 ± 0.87	38.12 ± 0.33
Ce	32.75 ± 0.38	32.88 ± 0.70	33.15 ± 1.72	45.73 ± 0.76
Nd	9.92 ± 0.60	9.74 ± 0.54	9.58 ± 0.35	13.30 ± 0.38
Sm	2.53 ± 0.28	2.54 ± 0.35	2.58 ± 0.08	2.83 ± 0.05

	OB100
La	30.76 ± 0.23
Ce	31.87 ± 0.58
Nd	9.19 ± 0.46
Sm	2.40 ± 0.13

Table 3.5 Results of obsidian samples with ICP-MS (Values are in mg/kg)

	OB 60	OB 62	OB 64	OB 66
La	26.49 ± 1.61	46.40 ± 6.03	23.33 ± 0.25	43.95 ± 5.18
Ce	49.19 ± 2.36	78.89 ± 8.14	45.09 ± 0.88	76.06 ± 8.04
Nd	14.47 ± 0.75	22.39 ± 2.31	13.33 ± 0.22	21.60 ± 2.37
Sm	2.30 ± 0.20	2.93 ± 0.50	1.96 ± 0.07	2.72 ± 0.45

	OB 68	OB 71	OB 72	OB 74
La	25.72 ± 3.30	28.41 ± 3.38	24.61 ± 0.44	30.98 ± 0.93
Ce	47.48 ± 3.70	51.83 ± 1.32	46.36 ± 0.57	56.15 ± 3.47
Nd	14.31 ± 1.28	15.47 ± 0.46	13.94 ± 0.18	17.15 ± 1.14
Sm	2.25 ± 0.27	2.40 ± 0.13	2.16 ± 0.03	2.83 ± 0.31

	OB 75	OB77	OB79	OB80
La	26.13 ± 1.97	27.52 ± 5.66	24.69 ± 1.70	25.76 ± 0.81
Ce	47.83 ± 2.43	47.98 ± 2.08	48.21 ± 3.50	49.53 ± 0.96
Nd	14.30 ± 0.76	14.30 ± 0.72	14.30 ± 1.11	14.64 ± 0.24
Sm	2.22 ± 0.22	2.16 ± 0.18	2.18 ± 0.18	2.17 ± 0.04

	OB 81	OB82	OB87	OB90
La	27.68 ± 0.93	26.67 ± 1.01	26.94 ± 1.29	26.25 ± 0.60
Ce	53.65 ± 1.67	51.74 ± 1.95	52.52 ± 2.52	50.91 ± 1.43
Nd	15.93 ± 0.42	15.32 ± 0.57	15.61 ± 0.90	14.80 ± 0.50
Sm	2.48 ± 0.12	2.33 ± 0.12	2.41 ± 0.22	2.28 ± 0.08

	OB91	OB92	OB93	OB97
La	27.69 ± 0.70	25.35 ± 1.79	27.59 ± 1.87	43.91 ± 4.55
Ce	53.96 ± 1.51	49.03 ± 3.60	53.00 ± 3.20	71.80 ± 3.90
Nd	15.79 ± 0.48	14.24 ± 1.11	15.53 ± 0.96	20.39 ± 1.24
Sm	2.49 ± 0.13	2.14 ± 0.27	2.37 ± 0.18	2.52 ± 0.22

	OB100
La	27.57 ± 0.21
Ce	53.92 ± 0.42
Nd	16.13 ± 0.06
Sm	2.54 ± 0.04

3.6.3. Normalized Spidergrams

Normalized spidergrams are constructed by using ratio of sample value to upper crust value of elements.

Upper crust element concentrations have been defined to compare other determinations in mostly geological research. These values serve as a reference point. Upper crust values of the elements used in this study are given in Table 3.6 [41].

Table 3.6 Upper Crust values (ppm)

Element	ppm
La	30
Ce	64
Nd	26
Sm	4.5

For the evaluation of the results, spidergrams of each obsidian sample were constructed and they were grouped according to the similar ratios of sample values to upper crust values. Then, the constructed spidergrams were matched with database [41] containing the spidergram of each obisidian source from

Çatalhöyük and its environment. The database is given in Figure 3.16. Constructed spidergrams are given in Figures from 3.11 to 3.15.

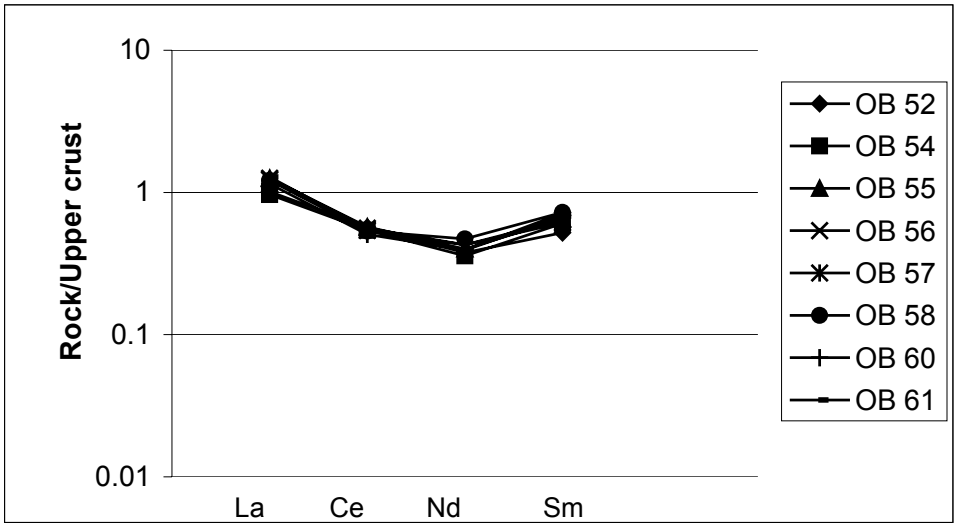

Figure 3.11 Obsidians from Acıgöl East Kartal-1

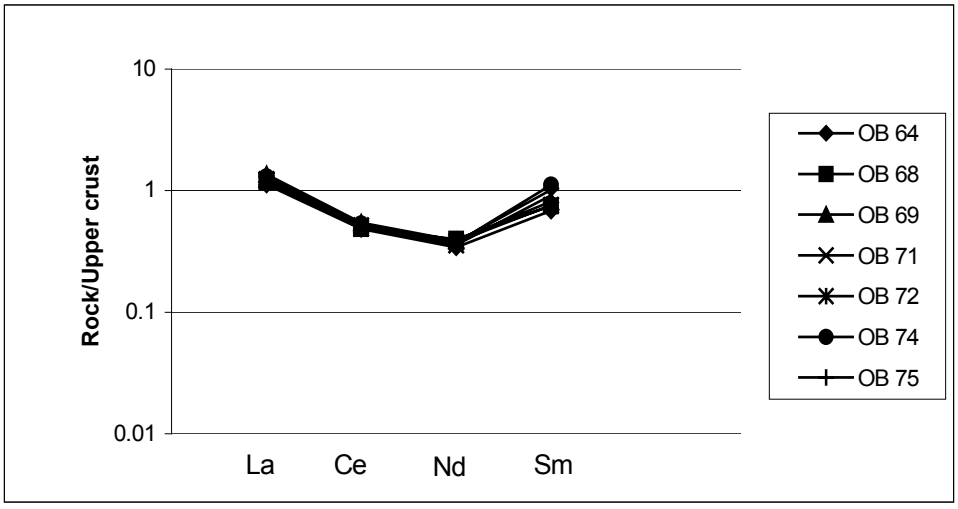

Figure 3.12 Obsidians from Acıgöl East Kartal-2

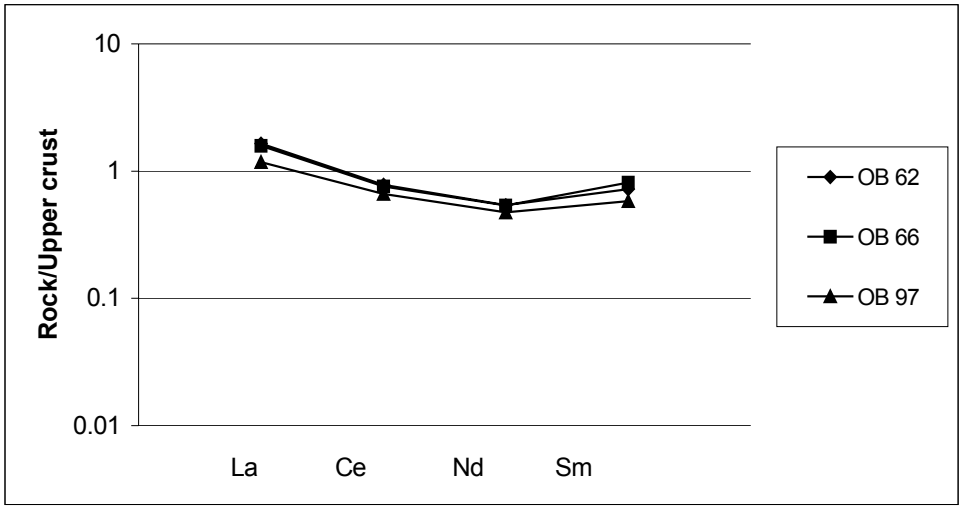

Figure 3.13 Obsidian from Nenezi Dağ

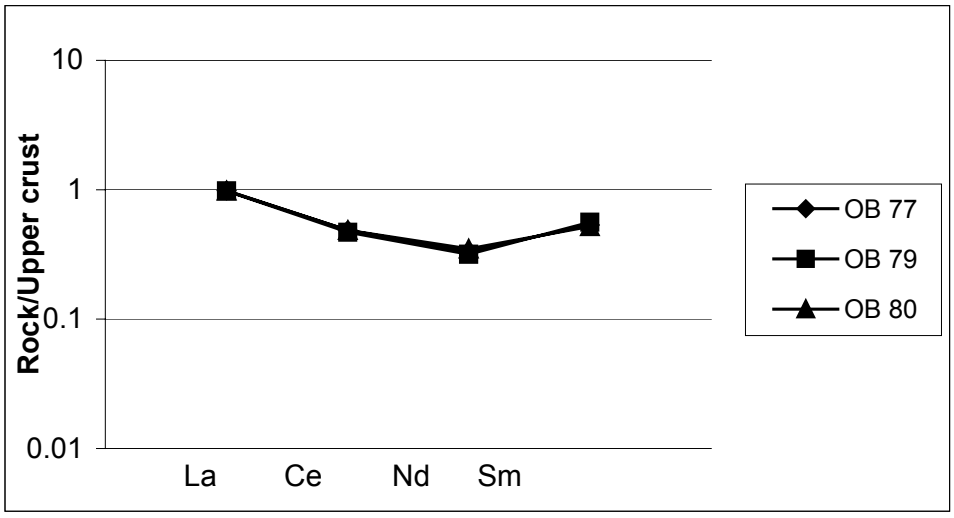

Figure 3.14 Obsidians from Acıgöl East Post Caldera

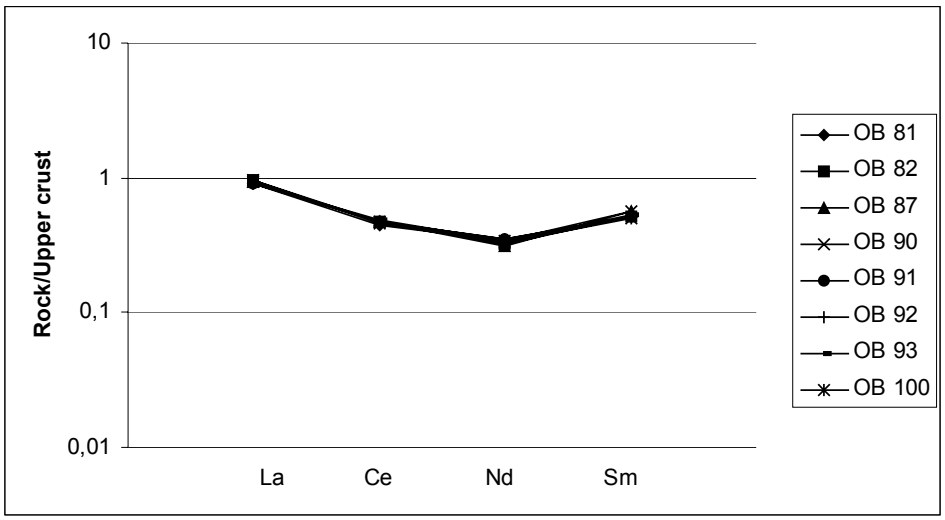

Figure 3.15 Obsidians from Göllü Dağ North Bozköy

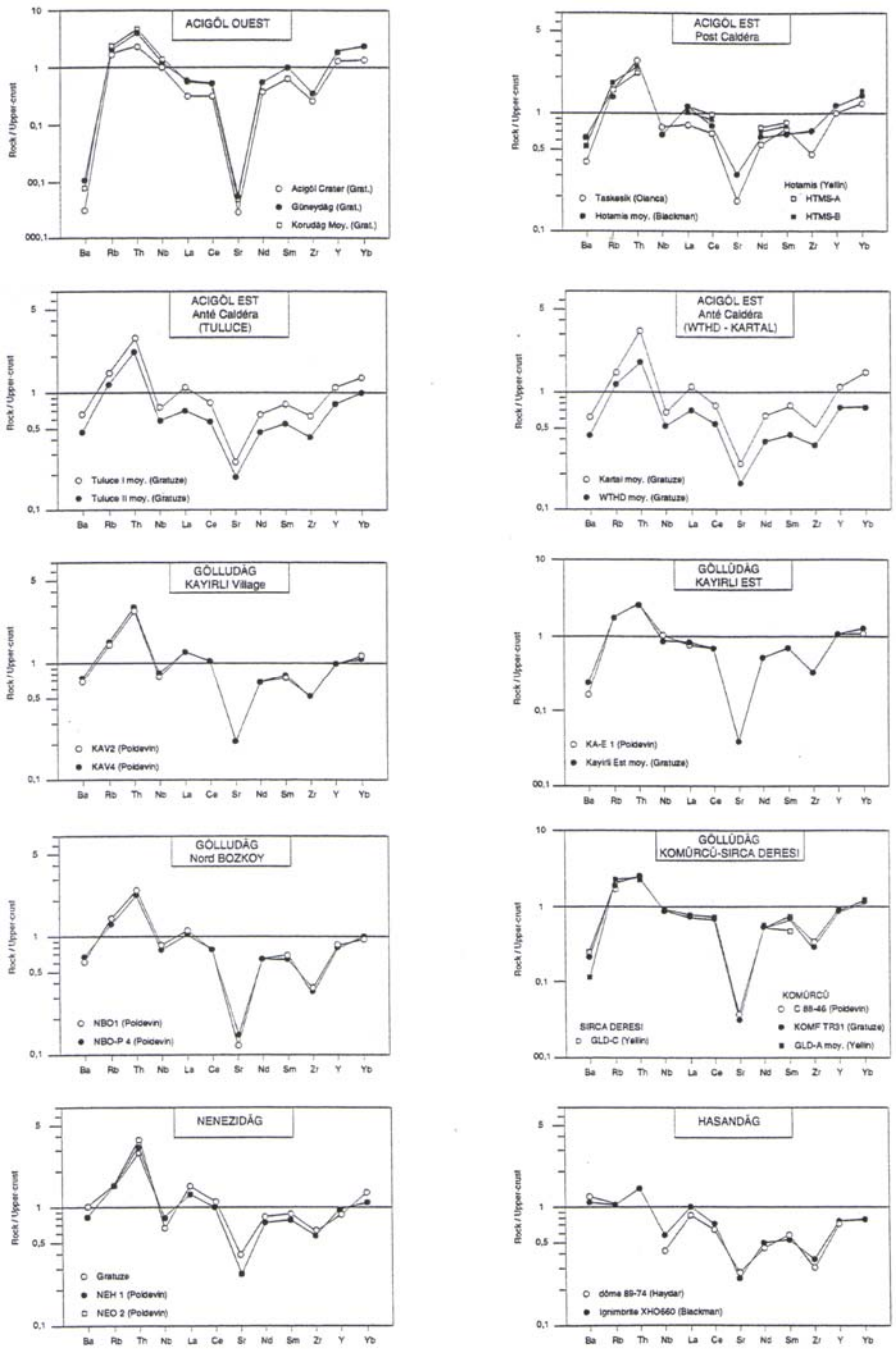

Figure 3.16 Normalized spidergrams of potential obsidian sources [42].

As a result of the normalized spidergrams (Figure 3.11,3.12) compared with the spidergrams given in Figure 3.16, OB52, OB54, OB55, OB56, OB57, OB58, OB60, OB61, OB64, OB68, OB69, OB71, OB72, OB74, OB75 belongs Acıgöl East Kartal.

OB62, OB66, OB97 (Figure 3.13) belongs Nenezi Dağ.

OB77, OB79, OB80 (Figure 3.14) belongs to Acıgöl East Post Caldere.

OB81, OB82, OB87, OB90, OB91, OB92, OB93, OB100 (Figure 3.15) belongs to Göllüdağ North, Bozköy.

CHAPTER IV

CONCLUSION

In this study, the applicability of the inductively coupled plasma atomic emission spectrometry for the analysis of obsidians sampled from Çatalhöyük excavations during 1999 summer was investigated. Solid-liquid extraction technique (SLE) was used for the pre-concentration of REE.

Different resins were examined and Amberlite IR-120 was chosen. For true REE concentrations in SARM-1 granite SRM, successive recovery results for each element was obtained. For the characterization studies, upper crust normalized diagram were used and results were compared with chemical composition of the sources. Although few of the trace elements were determined by ICP-OES, the results were enough to discriminate the samples. Normalized spidergrams and chemical compositions have very good correlation.

La, Ce, Nd and Sm elements in obsidian samples were also determined by ICP-MS in Hıfzıssıhha Institute of Izmir. ICP-MS and ICP-OES results did not correlate exactly, especially La and Ce.

Chemical composition of obsidian samples confirm that artefacts are from Göllüdağ North Bozköy, Nenezi Dağ, Acıgöl East Kartal, Acıgöl East Post Caldera sources.

REFERENCES

1. http://www.mineral.galleries.com
2. Thorpe W.O., Archaeometry, 37(2), (1995), 217-248
3. Pollard A.M., Heron C., Archaeological Chemistry, RSC paperbacks, Cambridge, (1996), pp. 84-90
4. Bellot-Gurlet L., Bigazzi G., Dorighel O., Oddone M., Poupeau G., Yegingil Z., Radiation Measurements, 31, (1999), 639-644
5. Brothwell D. , Higgs E., Clark G. (ed), Science in Archaeology, Thames and Hudson , City 1969, pp 578-591
6. www.turizm.net/turkey/history/history/neolithic.html
7. Edited by Roger Matthews, Ancient Anatolia, 1998, pp.35-51
8. http://catal.adrch.adc.uk/catal/mission.html
9. Abbes F., Bellot-Gurlet L., Cauvin M.C., Delerue S., Dubernet S., Poupeau G., Stordeur D., Journal of Non-Crystalline Solids, 323, (2003), 162-166
10. Chataigner C., Badalian R., Bigazzi G., Cauvin M.C., Jrbashian R., Karapetian S.G., Norelli P., Oddone M., Poidevin J.L., Journal of Non-Crystalline Solids, 323, (2003), 167-171
11. Duttine M., Villeneuve G., Poupeau G., Rossi A.M., Scorzelli R.B., Journal of Non-Crystalline Solids, 323, (2003), 193-199
12. Oddone M., Yegingil Z., Bigazzi G., Ercan T., Özdoğan M., Journal of Radioanalytical and Nuclear Chemistry, 224, (1997), 27-38
13. Bellot-Gurlet L., Calligaro Th., Dorighel O., Dran J.C., Poupeau G., Salomon J., Nuclear Instruments and Methods in Physics Research B, 150, (1999), 616-621
14. Elekes Z., Uzonyi I., Gratuze B., Rozsa P., Kiss A.Z., Szoor Gy., Nuclear Instruments and Methods in Physics Research B, 161-163, (2000), 836-841
15. Cotton F. Albert, Wilkinson Geoffrey, Advanced Inorganic Chemistry, John Wiley & Sons Inc, USA, (1988), pp 955
16. http://osoon.ut.ee/~hahha/re/history.html

17. Nachod F.C., Schubert Jack, Ion Exchange Technology, Academic press Inc., New York, (1956), pp 359-361
18. http://osoon.ut.ee/~hahha/re/general.html
19. Kantiipuly Chiran J., Westland Alan D., Talanta, 35, (1988), 1-13
20. Roychowdhury P., Roy N.K., Das D.K., Das A.K., Talanta, 36, (1989), 1183-1186
21. Srivastava P.K., Premadas A., Journel of Analytical Atomic Spectrometry, 14, (1999), 1087-1091
22. Halicz Ludwik, Gavrieli Ittai, Dorfman Ethel, Journel of Analytical Atomic Spectrometry, 11, (1996), 811-814
23. Texier A.C., Andres Y., Faur-brasquet C., Le Cloirec P., Chemosphere, 47, (2002), 333-342
24. Cai Bing, Hu Bin, Xiong Hongchun, Liao Zhenhuan, Mao Lesen, Jiang Zucheng, Talanta, 55, (2001), 85-91
25. Dev Kapil, Pathak Rita, Rao G.N., Talanta, 48, (1999), 579-584
26. Roelandts Iwan, Atomic Spectroscopy, 9, (1988), 49-54
27. Samuelson Olof, Ion Exchangers in Analytical Chemistry , John Wiley&Sons Inc., USA, (1953), pp1-3
28. Helfferich F., Ion Exchange, McGrow-Hill, New York, (1962),pp.35
29. Ingle J.D.Jr., Crouch S.R., Spectrochemical Analysis, Prectice Hall, USA, (1988), p.233-237
30. Skoog D.A., James J.J., Principles of Instrumental Analysis, Saunders College Publishing, USA, (1992),pp.233
31. Prasada R., Biju V.M., Critical Reviews in Analytical Chemistry, 30 (2&3), (2000), 179-220
32. Dennaud Jerume, Howes Adrian, Poussel Emmanuelle, Mermet Jean-Michel , Spectrochim. Acta Part B,56, (2001), 101-112
33. Chan George C., Chan Wing-Tat, Mao Xianglei, Russo Richard E., Spectrochim. Acta Part B,56, (2001), 77-92
34. Mermet J.M., Analytica Chimica Acta, 250 (1991), 85-94
35. Mermet J.M., Poussel E., Applied Spectroscopy, Vol-49, No:10, 1995, 12A-18A
36. http://www.rohmhaas.com/ioenexchange/amberlite.htm

37. Ayhan İ.Aysal., Provenance Studies in Obsidian Samples from Çatalhöyük Excavations, M.Sc. Thesis, METU (2002)
38. Mason Brian, Principles of Geochemistry, John Wiley & Sons, USA, (1958), p.30
39. Henderson Paul, Inorganic Geochemistry, Pergamon Press, London, (1984), pp.71-74
40. Volkan M., Ataman O.Y., Howard A.G., Analyst, 112, (1987), 1409-1412
41. Taylor S.R., McLennan S.M., The Continental Crust; Its Composition and Evolution, an Examination of the Geochemical Record Preserved in Sedimentary Rocks, Blackwell Scientific, 1985, p.29
42. Cauvin M.C., Gourgaud A., Poupeau G., Poidevin J.L., Chataigner C., L'obsidianne au Proche et Moyen Orient, BAR International Series 837, England,1998, p.124

APPENDIX-A

CALIBRATION CURVES

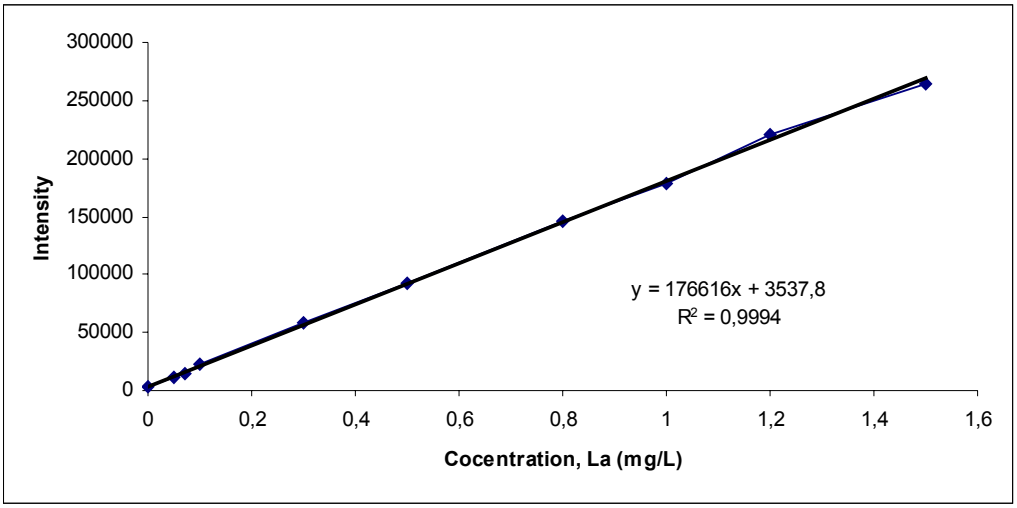

Figure A.1 Calibration curve for Lanthanum, 408.672 nm

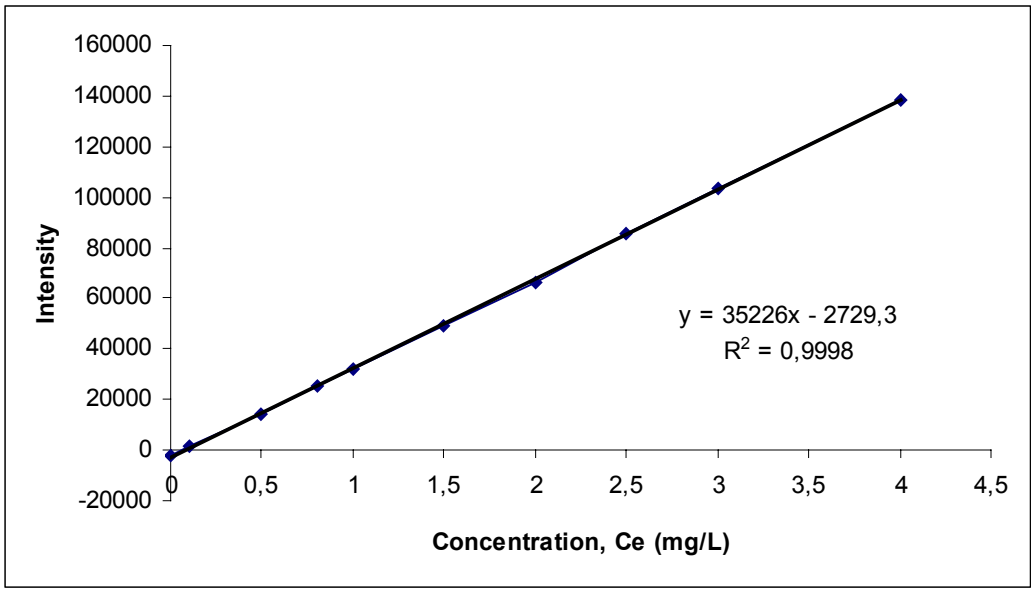

Figure A.2 Calibration curve for Cerium, 418.660 nm

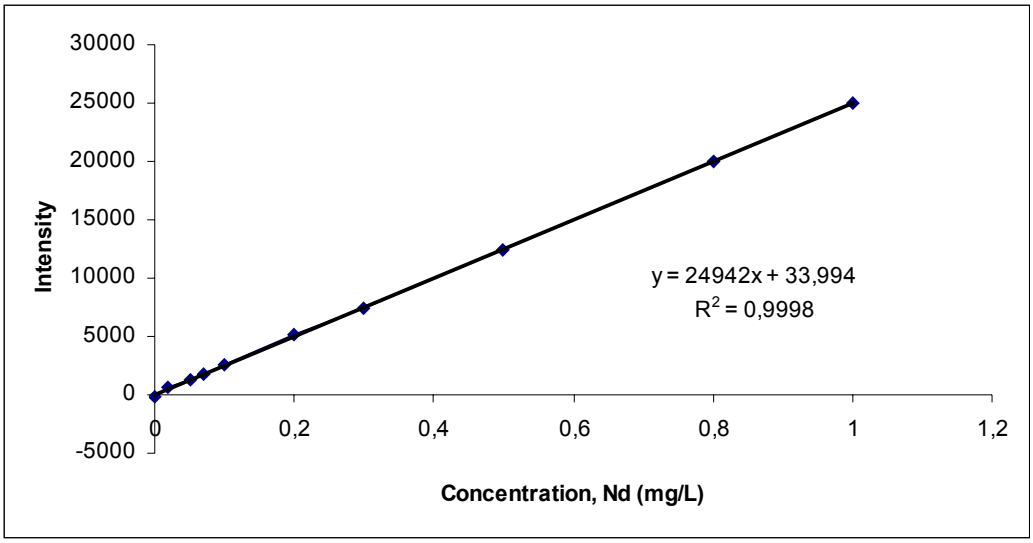

Figure A.3 Calibration curve for Neodymium, 415.608 nm

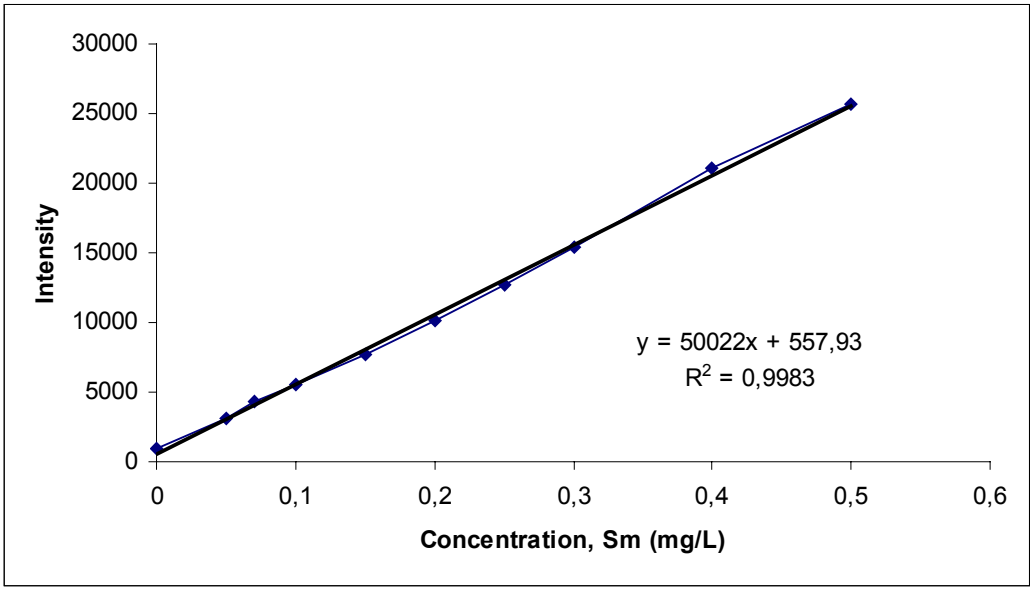

Figure A.4 Calibration curve for Samarium, 359.827 nm

APPENDIX-B

SAMPLE PICTURES

Figure B.1 Sample Picture OB51

Figure B.2 Sample Picture OB52

Figure B.3 Sample Picture OB53

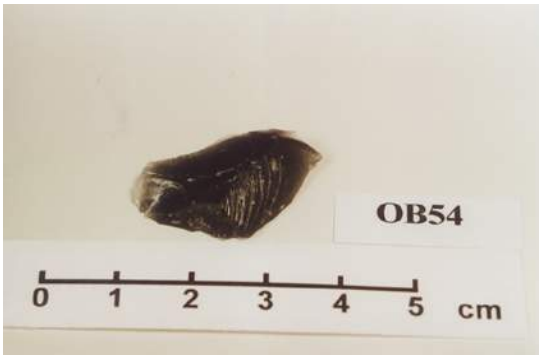

Figure B.4 Sample Picture OB54

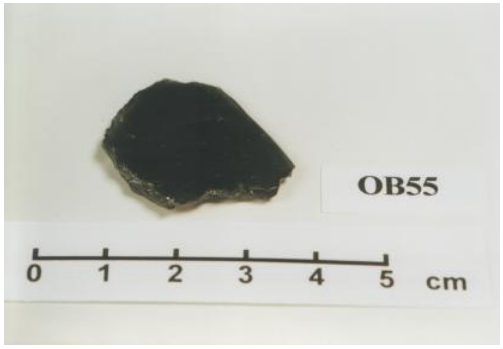

Figure B.5 Sample Picture OB55

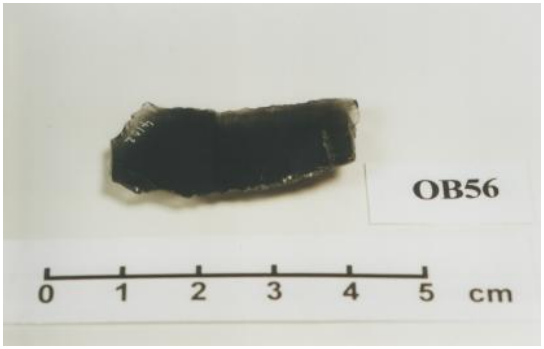

Figure B.6 Sample Picture OB56

Figure B.7 Sample Picture OB57

Figure B.8 Sample Picture OB58

Figure B.9 Sample Picture OB59

Figure B.10 Sample Picture OB60

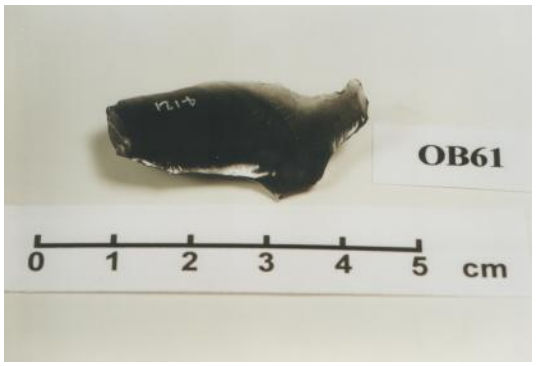

Figure B.11 Sample Picture OB61

Figure B.12 Sample Picture OB62

Figure B.13 Sample Picture OB63

Figure B.14 Sample Picture OB64

Figure B.15 Sample Picture OB65

Figure B.16 Sample Picture OB66

Figure B.17 Sample Picture OB67

Figure B.18 Sample Picture OB68

Figure B.19 Sample Picture OB69

Figure B.20 Sample Picture OB70

Figure B.21 Sample Picture OB71

Figure B.22 Sample Picture OB72

Figure B.23 Sample Picture OB73

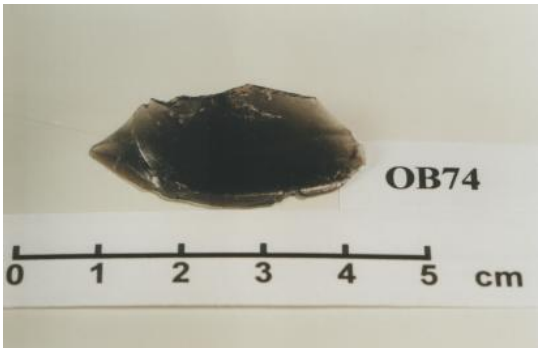

Figure B.24 Sample Picture OB74

Figure B.25 Sample Picture OB75

Figure B.26 Sample Picture OB76

Figure B.27 Sample Picture OB77

Figure B.28 Sample Picture OB78

Figure B.29 Sample Picture OB79

Figure B.30 Sample Picture OB80

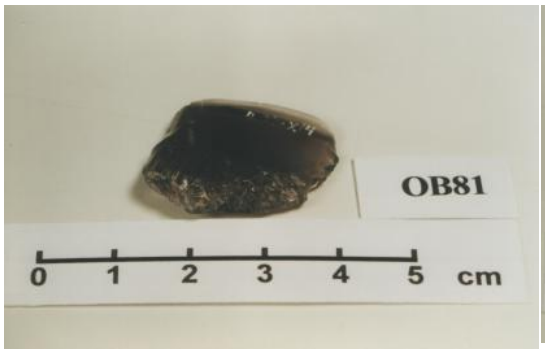

Figure B.31 Sample Picture OB81

Figure B.32 Sample Picture OB82

Figure B.33 Sample Picture OB83

Figure B.34 Sample Picture OB84

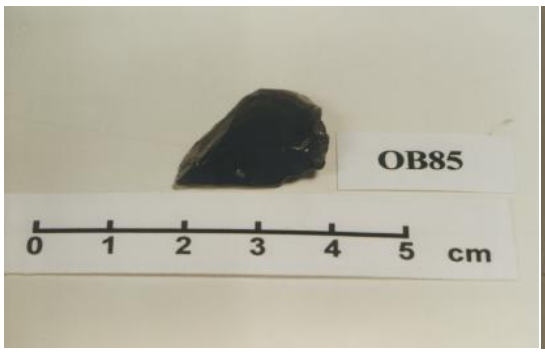

Figure B.35 Sample Picture OB85

Figure B.36 Sample Picture OB86

Figure B.37 Sample Picture OB87

Figure B.38 Sample Picture OB88

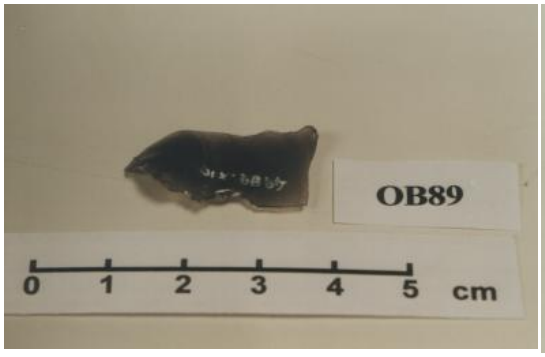

Figure B.39 Sample Picture OB89

Figure B.40 Sample Picture OB90

Figure B.41 Sample Picture OB91

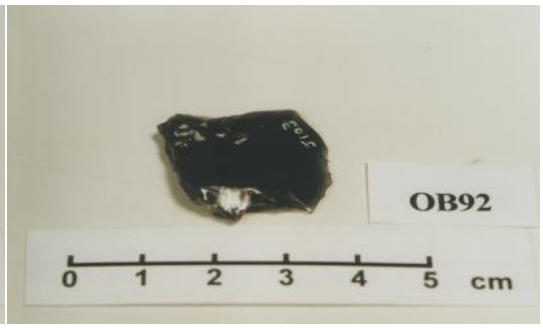

Figure B.42 Sample Picture OB92

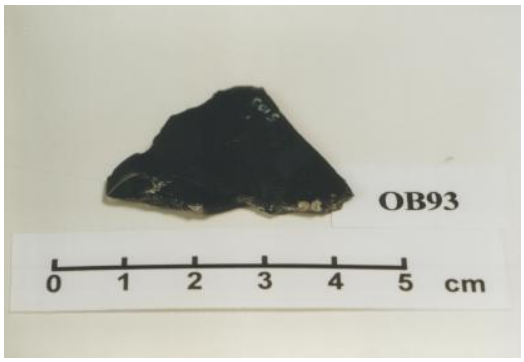

Figure B.43 Sample Picture OB93

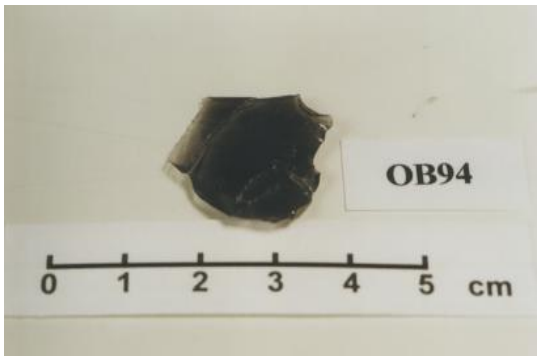

Figure B.44 Sample Picture OB94

Figure B.45 Sample Picture OB95

Figure B.46 Sample Picture OB96

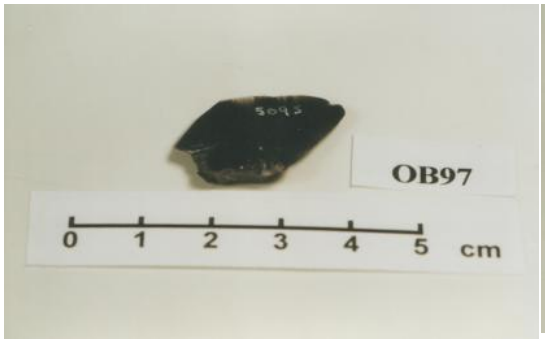

Figure B.47 Sample Picture OB97

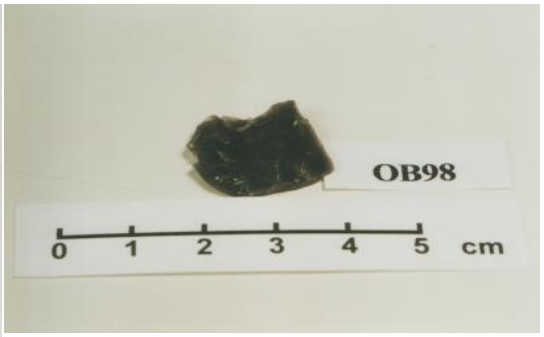

Figure B.48 Sample Picture OB98

Figure B.49 Sample Picture OB99

Figure B.50 Sample Picture OB100